2015

Synthesis of a C5'-pseudouridinyl radical precursor

Matthew J. Starr
University of Toledo

A Thesis

entitled

Synthesis of a C5′-Pseudouridinyl Radical Precursor

by

Matthew J. Starr

Submitted to the Graduate Faculty as partial fulfillment of the requirements for the

Master of Science Degree in

Medicinal Chemistry

_____

Dr. Amanda C. Bryant-Friedrich, Dr. rer. nat.
Committee Chair

_____

Dr. Zahoor Shah, Ph.D., Committee Member

_____

Dr. Donald Ronning, Ph.D., Committee Member

_____

Dr. Patricia R. Komuniecki, Dean
College of Graduate Studies

The University of Toledo

December 2015

An Abstract of

Synthesis of a C5′-Pseudouridinyl Radical Precursor

by

Matthew J. Starr

Submitted to the Graduate Faculty as partial fulfillment of the requirements for the
Master of Science Degree in
Medicinal Chemistry

The University of Toledo

December 2015

Reactive oxygen species can cause damage to proteins, lipids, and nucleic acids through the generation of free radicals. Oxidative damage in DNA has been studied quite extensively, with comparatively little work done on oxidative damage in RNA, which has been shown to play a role in Alzheimer's disease, Parkinson's disease and other neurodegenerative disorders. The goal of the project is to create a radical precursor that can be used to study oxidative damage in RNA, using pseudouridine, the most common modified nucleotide found in RNA. Introduction of a photolabile pivaloyl group at the C5′ site of pseudouridine will allow for the generation of a free radical at a specific position, leading to insights as to the mechanism of oxidative damage.

I dedicate this thesis to my parents for their unwavering support in my academic pursuits.

Acknowledgements

I would first and foremost like to acknowledge and thank my advisor, Dr. Amanda Bryant-Friedrich, for allowing me to join her research group and for all of her support. Without her guidance, knowledge, personal experience I would not be where I am at today.

I would like to thank my committee members for their support and involvement with this project.

Thank you to all of my lab members for their support and for sharing their chemistry knowledge and experience with me over the past few years, especially Matthew Ellis, and Dr. Fernand Mel Bedi. I have become a better scientist because of it. Thank you as well to my friends in other research groups for providing advice and assistance.

I would also like to thank my parents for their support and encouragement over the years. Thank you for believing in me even when I was doubting myself.

Table of Contents

List of Tables

List of Figures

List of Abbreviations

8-OHG.....8-hydroxyguanosine
8-OHdG .....8-Oxo-2´-deoxyguanosine

ACN .....Acetonitrile
AD .....Alzheimer's disease
ALS .....Amyotrophic lateral sclerosis

BACE-1 .....Beta-secretase 1

C .....Cytidine

DCM .....Dichloromethane
DIAD .....Diisopropyl azodicarboxylate
DMSO .....Dimethyl sulfoxide
DNA .....Deoxyribonucleic acid

EDC .....Reactive oxygen species
EtOAc .....Ethyl Acetate

GSH .....Glutathione

h .....Hours
HPLC .....High performance liquid chromatography
HRMS .....High resolution mass spectrometry

L-selectride .....Lithium tri-*sec*-butylborohydride
LC/MS .....Tandem liquid chromatography/ mass spectrometry

MALDI-TOF .....Reactive oxygen species
min .....minutes
mRNA .....Messenger ribonucleic acid

NADPH .....Nicotinamide adenine dinucleotide phosphate
NMR .....Nuclear magnetic resonance spectroscopy

OS .....Oxidative stress

PTC .....Reactive oxygen species

RNA .....Ribonucleic acid
rRNA .....Ribosomal ribonucleic acid
ROS.....Reactive oxygen species

SDS-PAGE .....Sodium dodecyl sulfate polyacrylamide gel electrophoresis
snRNA .....Small nuclear ribonucleic acid

TBAF .....Tetra-n-butylammonium fluoride
TBDMS .....*tert*-butyldimethylsilyl
TBDMSCN .....*tert*-butyldimethylsilyl cyanide
TBDPS .....*tert*-butyldiphenylsilyl
TFA .....Trifluoroacetic acid
THF .....Tetrahydrofuran
TLC .....Thin layer chromatography
TMS .....Trimethylsilyl
TMSCN .....Trimethylsilyl cyanide
tRNA .....Transfer ribonucleic acid

U .....Uridine
UV .....Ultra violet

List of Symbols

°C .....Degrees Celsius

BF_3-EtO_2 .....Boron trifluoride diethyl etherate

$CHCl_3$.....Chloroform

DMTr .....4,4´-dimethoxytrityl

M.....Molar

*n*BuLi .....*n*-butyl lithium

PPh_3.....Triphenylphosphine

*t*BuLi .....*tertiary*-butyl lithium
*t*BuSH.....*tertiary*-butyl lithium

$ZnCl_2$ .....Zinc chloride
ZnI_2 .....Zinc iodide

Chapter 1

Introduction

1.1 Naturally occurring modified nucleosides in RNA

Posttranscriptional modification of RNA is an important feature, allowing for a diversity of functions essential to cell life. Posttranscriptional modifications include splicing, or reordering of RNA, as well as modification of individual nucleotides by processes such as methylation. Many naturally occurring modified nucleosides have been discovered in recent years, with over 100 documented across all domains of life, and 66 occurring in eukaryotes. These modifications occur in mRNA, tRNA, rRNA, snRNA, and other types as well.[5] Many of the functions of these modifications are still a mystery, though some are known. These modifications could potentially alter RNA stability, translation, localization, trafficking regulatory capabilities, or other parameters.[6] RNA modifications have historically been difficult to detect, due to limits in technology, as well as the fact that reverse transcriptases used to synthesize RNA do not generally read these modified nucleosides differently.[6] Pseudouridinylation and 2′-O-methylation are by far the most numerous modifications.[7] Other common modifications include 6-methyl adenosine, 5-methyl cytosine, and inosine.[8]

Pseudouridine (**Figure 1-1**) was the first modified nucleoside to be discovered, and is the most abundant of all modifications that have been identified. This has resulted in pseudouridine being called the "fifth nucleoside".[9] It is an isomer of uridine, containing a C-C glycosyl bond as opposed to uridine's C-N glycosyl bond. Formation occurs enzymatically as a post transcriptional modification conducted by pseudouridine synthase. It is present in many structural RNAs, including tRNAs, where it is invariant.

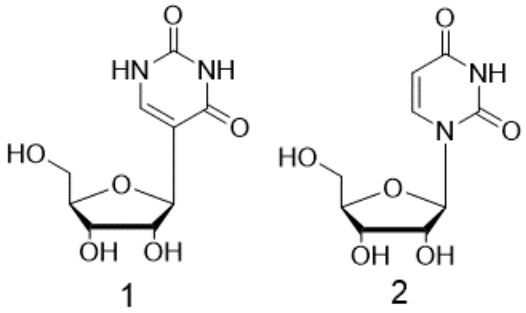

Figure 1-1 Pseudouridine (**1**) and uridine (**2**)

While the function(s) of this modification is not fully known, there is evidence to support several theories.[9] It could act as a conformational switch, allowing for different macro-structural possibilities than are available with uridine. It has the effect of rendering the RNA backbone more rigid, and may enhance the stability of secondary RNA structures.[7] Pseudouridine may also act as protection against chemical insult and radiation induced damage due to the more stable nature of its C-C linkage. Chemically, it possesses an extra hydrogen bond opportunity at the secondary N-1 position, potentially allowing for novel pairing interactions.[9] Pseudouridine also enhances base stacking.

Transfer RNAs are the most modified of all RNA. Approximately 15%-25% of all nucleosides in eukaryotic tRNA are modified in some way.[8] These modifications are theorized to be important for translational fidelity and tRNA distinction. Additionally, the

absence of inosine (**Figure 1-2**) at wobble position 34 causes decoding errors, as inosine can pair with uridine, adenine, and cytosine while adenine can only pair with uridine. Thus, tRNA modifications can directly affect the outcome of translation.

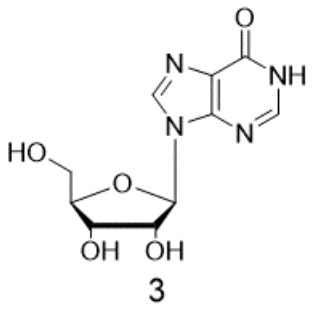

3

Figure 1-2 Inosine

Ribosomal RNA modifications include 91 pseudouridines, 105 2′-O-methylations and ten methylated bases. These modifications have been theorized to fine tune functional and structural properties of the ribosome or are perhaps involved in biogenesis.[8] This is supported by the fact that ribose favors the 3′-endo conformation as a result of 2′-O-methylation. One of the proposed theories as to the function of 2′-O-methylation is that it assists with interactions with tRNAs. Pseudouridine deficiencies in rRNA result in reduced translational fidelity, causing frame shift issues as well as issues reading stop codons.[10] Yeast strains that are deficient in rRNA modifications at the PTC showed altered peptidyl transferase rates and reduced translational fidelity, as well as changes in tRNA selection, offering some proof that these modifications are important for normal ribosomal function.

Modifications to mRNA mostly consist of methylations, due to the need for a lack of interference in the translation process. The primary sites of methylation are the N^7 of guanine, N^6 of cytosine, N^6 of adenosine and 2′-O-methylation of ribose. N^6-

methyladenosine is the most common eukaryotic mRNA modification, and it appears to be essential. There is evidence to suggest it could be part of the turn-over process in the cell, as mRNAs with this modification appear to have shorter half-lives.[8]

Modifications to other non-coding RNAs have also been discovered. Long noncoding RNAs, which are involved in mRNA processing, contain sites with N^6-methyladenosine. A component of the spliceosome, snRNAs, exhibit modifications that include pseudouridine, 2′-O-methylation, and N^6-methyladenosine. The function(s) of these modifications are not yet known.[8]

Modifications to RNA are numerous and enigmatic. They span across many different types of RNA and range in abundance between different transcripts. While the functions of these modifications are not fully understood, it is clear from evidence already obtained that many are of vital importance to normal, healthy cellular function.

1.2 Oxidative Damage in RNA

Oxidative damage is a constant occurrence in our cells. It can result in damage on a molecular level to such important biological molecules as nucleic acids, lipids, proteins, and sugars.[11] Oxidative insults can cause formation of adducts, dimers, and oxidation products to name a few. The chemical species that cause this oxidative damage are referred to as reactive oxygen species (ROS).

Sources of oxidative damage to cellular components (**Figure 1-3**) include: UV radiation from sunlight and artificial sources, free radicals, smoking, chemotherapeutic agents, growth factors, hyperthermia, and perhaps most importantly the cell itself. Radicals are formed as part of the normal function of the electron transport chain in cellular respiration, which occurs within the mitochondria.[12] One of the main radicals formed during this process is the superoxide radical. Radicals are also produced by the endoplasmic reticulum and nuclear membranes as a result of oxidative phosphorylation.[13] Other deleterious ROS include the hydroxyl radical (the most reactive) and hydrogen peroxide. Enzymes can also produce ROS as a by-product of their metabolic activity. Metabolism of arachidonic acid by cyclooxygenase, lipoxygenase, and cytochrome P450 mono-oxygenase is known to produce ROS, as are the enzymes xanthine oxidase and NADH/NADPH oxidase.[13]

RNA is much more likely than DNA to experience oxidative insult for several reasons. It is much more abundant in the cell than DNA in terms of total amount. Location is also a factor; DNA is protected inside the nucleus of the cell, while RNA is distributed throughout the cellular cytoplasm, bringing it into closer proximity to

potentially damaging chemical species such as those produced in the mitochondria. The single stranded nature of (most) RNAs make them much less stable than DNA duplexes due to the lack of hydrogen bonding that help protect the nucleobases from insult. RNA also lacks the specific binding proteins that DNA has.[14] These factors indicate that oxidative insult to RNA likely occurs much more frequently than to DNA. However, the majority of the work done in this field has focused on DNA, with comparatively little work being done on RNA. Of the studies published on RNA, most of the work has focused on base damage as opposed to sugar damage.

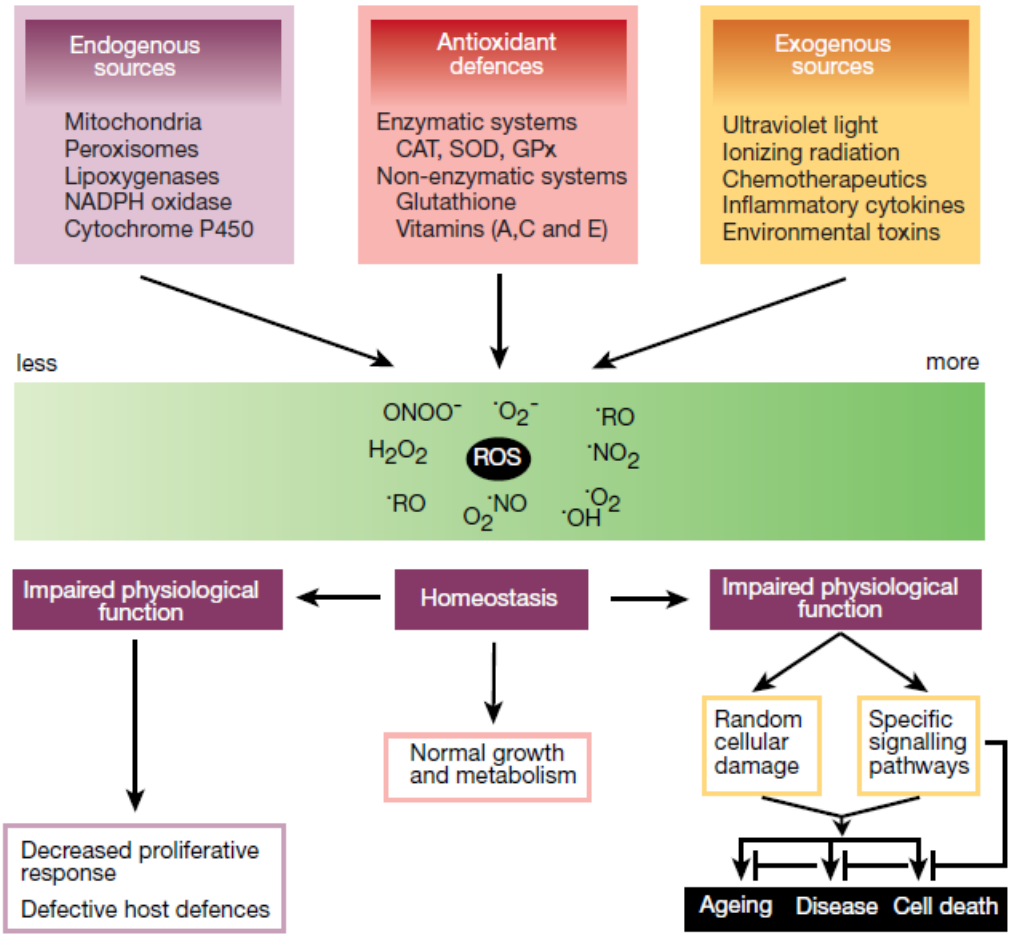

Figure 1-3 Sources of ROS. "Holbrook, T.F.a.N.J., Oxidants, oxidative stress and the biology of ageing. Nature, 2000. **408**(9): p. 239-247." Reprinted with permission.

Because the cell itself regularly produces chemical species capable of this damage, there exist protection mechanisms that the cell can utilize to minimize damage. One of the main mechanisms of protection involves glutathione (GSH), which is an antioxidant and a tripeptide present in animal cells. Glutathione is a reducing agent, and forms glutathione disulfide in its oxidized form. GSH can be regenerated using NADPH as a source of hydrogen atoms. The ratio of reduced/oxidized glutathione can serve as an indicator of cellular toxicity levels in a clinical setting. Other antioxidants that afford some protection to the cell are both enzymatic and non-enzymatic in nature, and include flavonoids, superoxide dismutase, catalases, Vitamin C, Vitamin E and glutathione peroxidase. [11, 15] When these defense mechanisms get overwhelmed by high levels of ROS, the cell is said to be under "oxidative stress".

Superoxide dismutase is the enzyme that catalyzes the formation of hydrogen peroxide from super oxide radicals. Hydrogen peroxide is degraded enzymatically to water and oxygen under normal conditions, however it is capable of reacting with intracellular iron (Fe^{2+} and Fe^{3+}) to undergo a series of radical reactions, resulting in the production of damaging ROS that includes the hydroxyl radical in processes called the Haber-Weiss and Fenton reactions (**Figure 1-4**).[13]

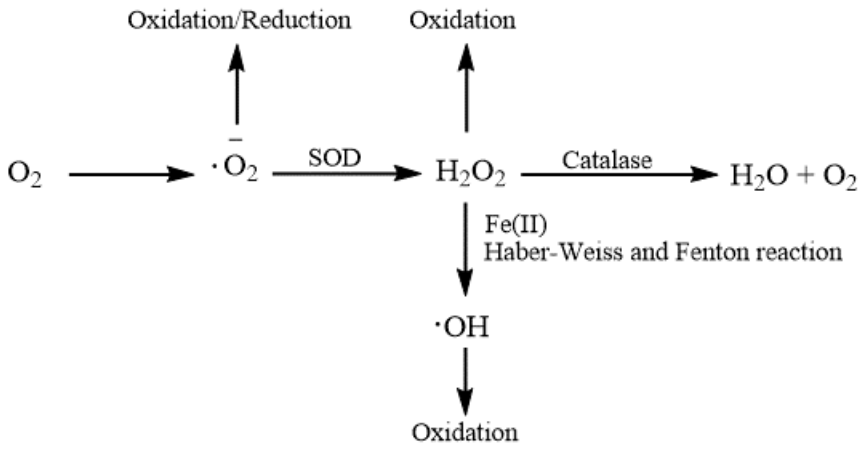

Figure 1-4 Formation and fate of a superoxide radical.

UV radiation can cause different types of damage to RNA. In experiments done by irradiating synthetic poly(U) and poly(C) RNAs it was found that cyclobutane pyrimidine dimers form, as do uridine hydrate and cytidine hydrate (**Figure 1-5**).[16] It was found during these studies that single-stranded RNA is more susceptible to photo-damage than double-stranded RNA. It is not clear if these observed products occur *in vivo*; early studies were performed using UVC radiation, which is biologically irrelevant due to the protective ozone layer of the atmosphere preventing its reaching earth's surface.

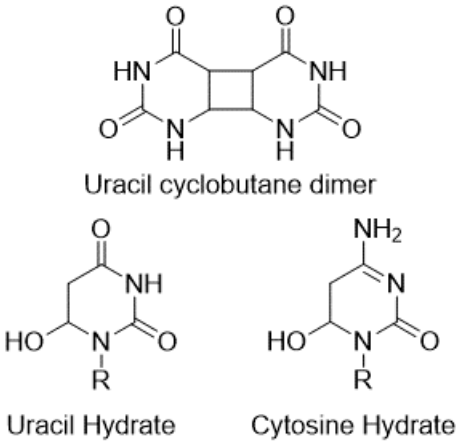

Figure 1-5 Photodamage products

One of the most well-known oxidative damage products is 8-oxoguanine, which occurs in both DNA (as 8-OHdG) and RNA (8-OHG) (**Figure 1-6)** as the most common lesion in cells under oxidative stress. It can be used as a marker to determine the extent of oxidative damage using antibodies to isolate RNAs exhibiting this modification. In this manner, it was found that RNA experiences a greater degree of oxidative damage under induced oxidative stress than does DNA. This technique also provided evidence that RNA susceptibility to oxidative insult varies between coding and non-coding RNAs, as well as between different mRNAs. This may be a result of the differing degrees of protein

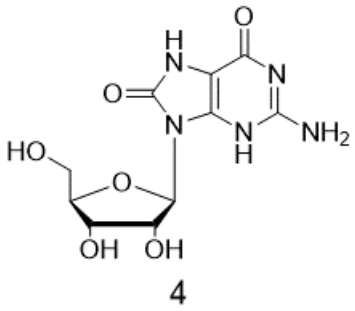

Figure 1-6 8-OHG

association between RNAs, though it is not yet completely clear.[16] 8-OHG is capable of pairing with both adenine and cysteine, compromising the integrity of the translation process and leading to proteins that can end up misfolded or non-functional. Overall, more than twenty oxidatively modified nucleotides have been discovered, with other major species including 8-hydroxyadenosine, 5-hydroxycytidine, and 5-hydroxyuridine; these modifications may also exhibit non-canonical pairing options, just as 8-OHG does.[17]

Certain sites in RNA may be more susceptible to oxidative insult than others. One factor is the neighboring nucleosides, which can contribute to the reactivity in some cases. Protein association may be another factor.[16] As already stated, association with intracellular iron increases susceptibility to oxidation. A study done using ammonia-treated rat astrocytes found rRNA and some mRNAs were oxidized, while some mRNAs were not. This may be a result of chemical factors, or perhaps different mRNAs are preferentially repaired or degraded over others resulting in a lack of detection of these species.[16]

1.3 Oxidative damage in RNA and relevance to disease

Oxidative stress (OS) and oxidative damage to RNA have been implicated in a number of psychological disease states, including Alzheimer's disease, Parkinson's disease, amyotrophic lateral sclerosis, Huntington's disease and vascular dementia [11, 14, 15]. There is also evidence oxidative stress could be a risk factor for cardiovascular issues such as angina and myocardial infarction.[13] The brain is particularly susceptible to the effects of oxidative stress due to its richness in fatty acids, consumption of large amounts of oxygen, and a lack of antioxidant activity. It is not clear if OS is the cause of or the effect of neurodegeneration, but certainly plays a role in the events leading to neuron death.[11]

Alzheimer's disease is the leading cause of dementia in the elderly, second most costly disease after cancer, and the fourth most common cause of death in the western world. Alzheimer's disease is characterized by brain atrophy, neurofibrillary tangles and neural plaques. Parkinson's disease results in tremors and other motor symptoms such as bradykinesia due to degeneration of dopamine-producing neurons in the substantia nigra of the basil ganglia in the brain. The occurrence of AD in the United States is 67 per 1,000 elderly, and 9.5 per 1,000 elderly for Parkinson's disease.[17] Dementia is a common symptom in advanced stages of the disease. Huntington's disease is a heritable neurodegenerative disorder with onset generally occur in middle age. The hallmark of the disease is abnormal involuntary movements called chorea, and coordination/movement as well as psychiatric problems. Medical imaging of patients with Huntington's disease shows atrophy of the caudate nuclei and striatal volume. ALS can be either familial or

sporadic and is assumed to be a result of damage to motor neurons in the primary motor cortex corticospinal tract, brain stem, and spinal cord.[15]

Aggregation of misfolded proteins is a major feature of neurodegenerative disease. It has been found that oxidative stress conditions increase the amount of protein aggregation in the cell. Neurofibrillary tangles and amyloid-β plaques are characteristic of Alzheimer's disease. Oxidative stress has been shown using *in vitro* models to result in hyperphosphorylation of micro-tubule associated protein Tau, the major component of neurofibrillary tangles. Phosphorylated Tau (and other cytoskeletal proteins) are vulnerable to modification by carbonyl products of oxidative stress, resulting in aggregation into fibrils.[15] Phosphorylated Tau can be modified by 4-hydroxy-2-nonenal resulting in a conformation change that contributes to the formation of fibrils.[15] Amyloid-β plaques are a result of abnormal enzymatic activity that cleaves (using BACE1) amyloid precursor protein into a 39-43 amino acid peptide, called amyloid-β, which forms clumps deposited outside of neurons called plaques. Exposure to hydrogen peroxide in human neuroblastoma cells results in an increase in plaque formation.

Increased oxidation of RNA, as well as DNA, has been observed in the post-mortem brains of Alzheimer's disease patients, with mRNA being oxidized in the range of 30%-70% compared to 2% in age matched controls.[18] Oxidation also increases in tRNA and rRNA in Alzheimer's, with rRNA presenting with 13 times as much 8-OHG as tRNA. In neurons, rRNA is extremely abundant; it also demonstrates higher binding capacity to redox active iron, accounting for the increased oxidation of rRNA as compared to other species of RNAs. Studies on oxidatively damaged ribosomes has shown decreases in protein production.[18, 19] Increases in lipid peroxidation products

have also been seen in neurodegenerative diseases.[20] Experiments done using RNase pretreatment showed a great decrease in immunoreactivity of 8-OHG/8-OHdG, showing that the oxidation was mainly occurring in RNA; using immunoelectron microscopy it was observed that oxidized nucleosides were mostly localized to the ribosome. [20] Ribosomes from the hippocampus of AD patients contain much higher levels redox-active iron, which is bound to rRNA. Ribosomal RNA is likely oxidized by the hydroxyl radical, however it is not readily diffusible through tissue. Hydrogen peroxide is quite diffusible, and coupled with the increased redox-active iron bound to rRNA, it is quite possible that the Fenton reaction is generating hydroxyl radicals from hydrogen peroxide. Mitochondrial disruption also likely plays a role in the increased abundance of ROS seen in AD (**Figure 1-7**).[20]

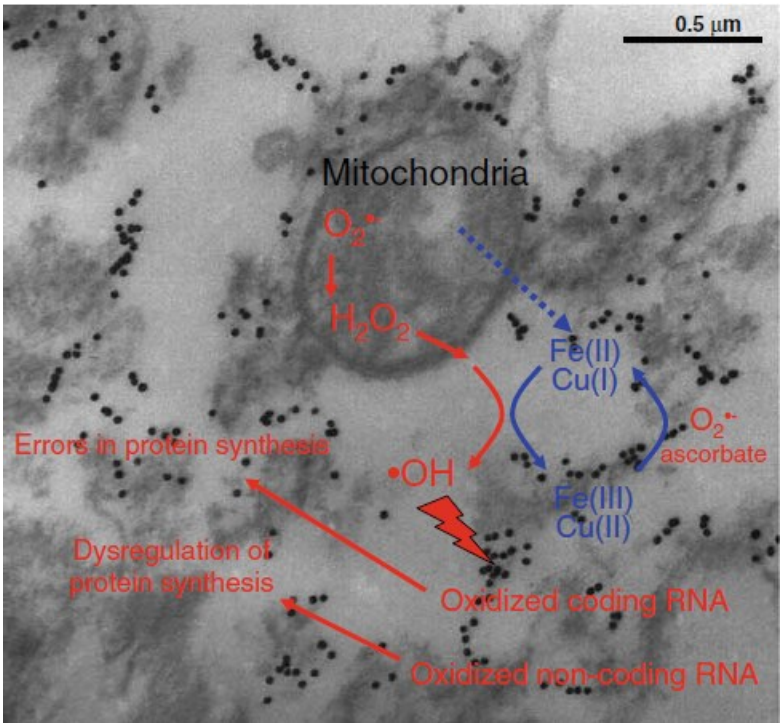

Figure 1-7 "Disrupted mitochondria likely play a role in ROS production and supplying redox-active metals that catalyze OH radical production. Background immunoelectron micrograph shows cytoplasmic 8-OHG immunolabeling (colloidal gold) with ribosomal pattern of distribution in a neuron of the AD brain." Nunomura, A., et al., *RNA oxidation in Alzheimer disease and related neurodegenerative disorders.* Acta Neuropathol, 2009. **118**(1): p. 151-66. Reprinted with permission

The distribution of RNA oxidation in the brain differs depending on which disease the brain is suffering. In Alzheimer's, the hippocampus and cerebral neocortex exhibit increases. In Parkinson's disease, the substantia nigra shows increased oxidation. Oxidized RNA has been found in the motor cortex and spinal cord of patients with ALS. No alteration of 8-OHG levels has been seen in the cerebellum in any of these disorders. [20]

High levels of oxidation of RNA is a commonly exhibited symptom in neurodegenerative disorders, and has disastrous effects on neuronal cells. Oxidative stress has been implicated as a key player in the reduced protein expression, protein misfolding,

and protein aggregation seen in these diseases. While the exact role of RNA oxidation in neurodegenerative disease is not completely clear, it is certain that it has a key role in the mechanism leading to neuron death.

1.4 Investigational Methods into RNA oxidation

Investigating RNA oxidation has resulted in several methods to determine the extent of oxidative stress and to model the damage that occurs by radical attacks. Methods for determining the extent of oxidative stress have used immunochemistry to isolate oxidized RNAs exhibiting 8-OHG using antibodies coupled with SDS-PAGE techniques to separate the isolated RNAs. The isolated RNAs can be quantified and characterized using mass spectrometry analysis, among other techniques. These types of analyses can be performed on samples such as tissue from the brain of an Alzheimer's or Parkinson's patient. This allows researchers to study these diseases on a molecular level, potentially allowing for identification of oxidatively damaged RNAs that are important to the disease etiology.

Radical precursors have also been developed to model oxidative damage by generating a radical at a specific position on the nucleoside sugar ring or base. These radical precursors are made using synthetic organic chemistry to install special photolabile groups, such as a phenyl selenium or pivoloyl group that can be photolyzed using UV radiation at biologically relevant wavelengths, ≥320 nm (UVA), and undergo Norrish Type I photo cleavage.

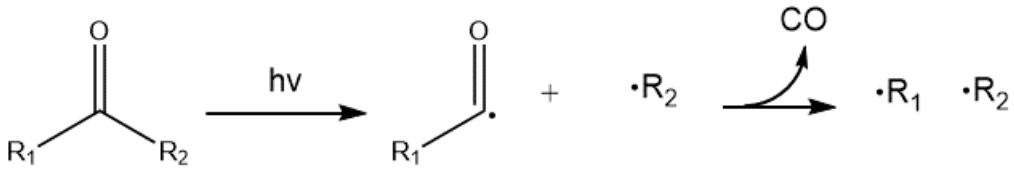

Figure 1-8 Norrish type I photocleavage

Greenberg's group used a C-6 uridinyl radical precursor (**Figure 1-8**) to show that a C-6 radical can abstract a 2′-hydrogen from a neighboring nucleotide, resulting in a strand break at the 3′-phosphate. [21] This is a result of the significantly lowered bond dissociation energy of the 2′-H in RNA as compared to DNA, a result of the 2′-OH present in ribose.[22]

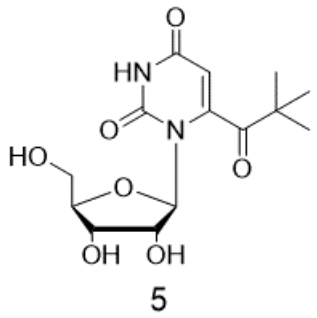

5

Figure 1-9 Greenberg's C6-uridinyl radical precursor

Chatgilialoglu's group synthesized C5′ *tert*-butyl ketone derivatives of thymidine and 2′-deoxyguanosine to act as photolabile radical precursors (**Figure 1-9**). The C5′ site was chosen due to its accessibility for hydrogen abstraction by a hydroxyl radical. Hydrogen atom abstraction at this position can result in the formation of 5′,8-cyclonucleosides.[23] They concluded that the fate of a C5′ radical is dependent upon the structure of the base. The thymidine radical was effectively reduced by a physiologically

relevant concentration of alkane thiol, while the guanosine analogue adds intramolecularly to the C8-N7 double bond.[23] Tullius's group found that a hydroxyl radical is capable of abstracting a hydrogen atom from the 5′ position of ribose, resulting in strand scission and formation of a 5′-aldehyde.[24]

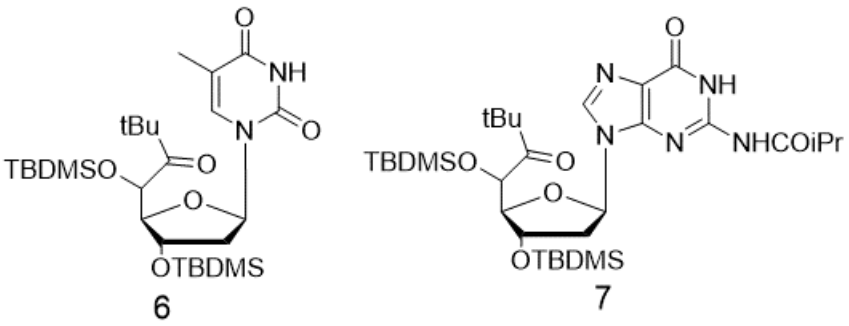

Figure 1-10 Chatgilialoglu's radical precursors

In this work, we present the synthesis of a C5′ pseudouridinyl radical precursor. To our knowledge, it is the first pseudouridine radical precursor that has been synthesized, and holds great potential in determining the fate of a radical insult to pseudouridine. This molecule would also allow for derivatization for automated oligonucleotide synthesis, allowing for the determination of the effect of a pseudouridinyl radical would have on RNA sequences.

Chapter 2

Experimental Section

2.1 General Methods

Reactions were carried out under standard laboratory conditions. Where exclusion of water and/or oxygen is necessary high-purity argon gas was used directly without further purification to create an inert atmosphere. Moisture and oxygen sensitive compounds were transferred by syringe to maintain inert conditions. All glassware was oven dried unless otherwise indicated.

Materials

All reagents were purchased commercially and used without further purification. Solvents were purchased from Fisher Scientific and Sigma-Aldrich and were ACS reagent grade unless otherwise indicated. Anhydrous THF was obtained by distillation over sodium and benzophenone and used immediately for best results. Deuterated solvents for NMR were purchased from Cambridge Isotope Laboratories.

2.2 Synthesis of C5'-pivaloyl pseudouridine

2.2.1 Synthesis of (3aR,6R,6aR)-6-(((tert-butyldiphenylsilyl)oxy)methyl)-4-(2,4-di-tert-butoxypyrimidin-5-yl)-2,2-dimethyltetrahydrofuro[3,4-d][1,3]dioxol-4-ol

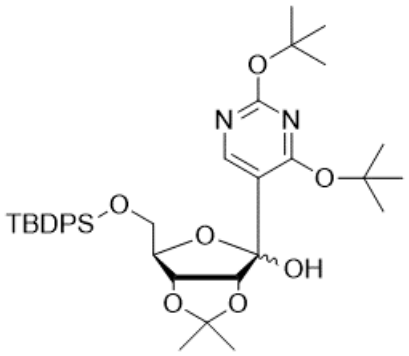

8

Compound **11** (2.73g, 9 mmol) was added to a 3-necked round bottom flask equipped with a magnetic stir bar. The system was purged with dry Ar gas, and 95 ml dry THF added with stirring to dissolve the reactant. The solution was cooled to -78 °C using a dry ice/acetone bath for about 30 min, at which time *n*BuLi solution (6.2 ml, 9.9 mmol; 1.6 M in hexanes) was added dropwise. After allowing to react for 1h, a solution of **12** (1.99 g, 4.67 mmol) in THF (35 ml) was cannulated into the reaction solution. Maintaining reduced temperature, the reaction was allowed to proceed for 2.5 hours, at which point it was determined to be complete by TLC (15% EtOAc/Hexanes mobile phase). The reaction was quenched using 53 ml of brine and allowed to thaw. The aqueous layer was extracted with EtOAc (75 mlx4). The combined organic layers were dried using magnesium sulfate, and concentrated under reduced pressure. The crude was purified by flash chromatography (EtOAc/Hexanes gradient 15-40%) to obtain **4** (2.06 g, 3.17 mmol) in 68% yield. Characterization and spectra available.[25]

2.2.2 Synthesis of (1S)-2-((tert-butyldiphenylsilyl)oxy)-1-((4S,5R)-5-((2,4-di-tert-butoxypyrimidin-5-yl)(hydroxy)methyl)-2,2-dimethyl-1,3-dioxolan-4-yl)ethan-1-ol

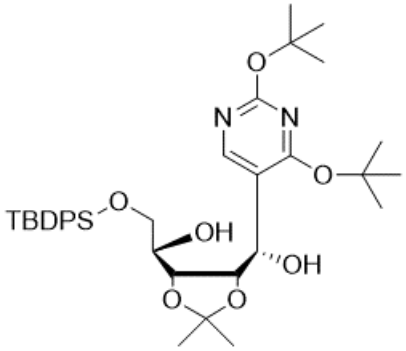

9

Compound **8** (1.4 g, 2.55 mmol) was added to a clean, dry 3 necked round bottom flask equipped with a magnetic stir bar. The flask was purged with dry argon gas, and the reactant dissolved in dry DCM (95 ml). The solution was cooled to -78 °C using a dry ice/acetone bath, after which a $ZnCl_2$ solution (3.8 ml) was slowly added and the reaction was left to stir for 40 min. L-selectride solution (8.9 ml) was added slowly, and left to react overnight. After about 17 h the reaction was determined to be complete by TLC (20% EtOAc/Hexanes) and quenched with methanol (2.5 ml), water (2.5 ml), H_2O_2 (2.5 ml), and NaOH (2.5 ml, 6M solution). The aqueous layer was extracted with EtOAc (30 ml x 3), and the combined organic layers dried over magnesium sulfate. The crude was purified by flash chromatography to obtain compound **9** (1.11 g, 1.7 mmol) in 67% yield. Characterization and spectra available.[25]

2.2.3 Synthesis of 2,4-di-tert-butoxy-5-((3aS,4S,6R,6aR)-6-(((tert-butyldiphenylsilyl)oxy)methyl)-2,2-dimethyltetrahydrofuro[3,4-d][1,3]dioxol-4-yl)pyrimidine

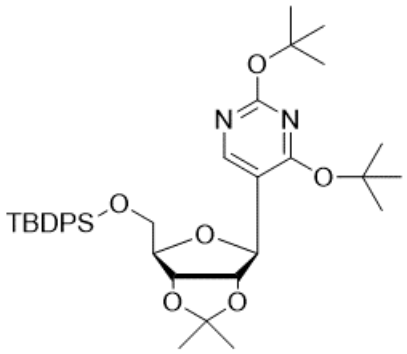

10

Compound **9** and triphenylphosphine (.769 g, 2.88 mol) were transferred to a clean, dry round bottom flask and co-evaporated from toluene. The flask was equipped with a stir bar and purged with dry argon gas. Anhydrous THF (25 mL) was added to the flask with stirring to dissolve all solids. The solution was cooled to 0 °C in an ice bath, DIAD (.60 mL, 3.05 mmol) was added and the reaction left to stir for 22 h. The reaction mixture was concentrated and the crude product was purified by flash chromatography on silica gel (30% EtOAc/Hex) to obtain compound **10** (610 mg, 1.43 mmol) in 99% yield. Characterization and spectra available.[25]

2.2.4 Synthesis of ((3aR,4R,6S,6aS)-6-(2,4-di-tert-butoxypyrimidin-5-yl)-2,2-dimethyltetrahydrofuro[3,4-d][1,3]dioxol-4-yl)methanol

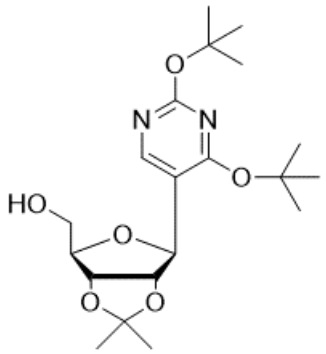

11

Compound **10** (290 mg, .45 mmol) was transferred to clean, dry round bottom flask equipped with a stir bar and dissolved in dry THF under inert atmosphere. The solution was cooled to 0 °C and TBAF (.68 mL, .68 mmol, 1M solution in THF) was added dropwise. The reaction mixture was warmed to room temp and stirred for 2.5 h, at which point it was deemed complete by TLC (25% EtOAc/Hex). The compound was purified by flash chromatography (25%-100% EtOAc/Hex gradient) to obtain compound **11** (170 mg, 0.43 mmol) in 96% yield. Characterization and spectra available.[25]

2.2.5 Synthesis of (3aS,4S,6S,6aS)-6-(2,4-di-tert-butoxypyrimidin-5-yl)-2,2-dimethyltetrahydrofuro[3,4-d][1,3]dioxole-4-carbaldehyde

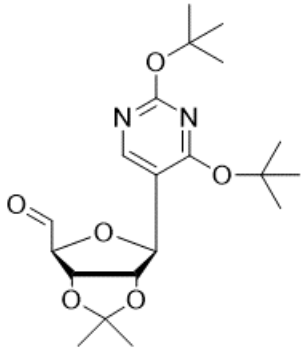

12

Compound **11** (.463 g, 1.17 mmol) and solid EDC (.544 g, 3.51 mmol) were co-evaporated from toluene. The flask was equipped with a stir bar and purged with dry argon gas. The solids were dissolved in Toluene (7 mL) and DMSO (3.5 mL) with stirring. To the stirred solution was added pyridine (.33 mL, 4.1 mmol) and TFA (0.05 mL, 0.59 mmol). The reaction mixture was allowed to stir and monitored for completion by TLC (1:1 EtOAc/Hex). The reaction was deemed reaction complete after 4h and diluted with $CHCl_3$, then washed with water (10 mL) and then brine (10 mL). The combined organics were dried over sodium sulfate and concentrated under reduced pressure. Obtained compound **12** which was used immediately without purification. Characterization and spectra available.[25]

2.2.6 Synthesis of 2-((tert-butyldimethylsilyl)oxy)-2-((3aR,4S,6S,6aS)-6-(2,4-di-tert-butoxypyrimidin-5-yl)-2,2-dimethyltetrahydrofuro[3,4-d][1,3]dioxol-4-yl)acetonitrile

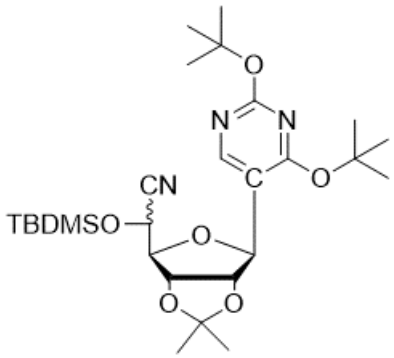

13

Compound **12,** TBDMSCN (393 mg, 2.79 mmol), and a spatula tip of ZnI_2 was dissolved in anhydrous DCM (6 mL) under an inert atmosphere. The reaction was stirred for 18 h and additional TBDMSCN (165 mg, 1.17 mmol) was added. The reaction was allowed to run 3 days, then diluted with DCM (10 ml). The reaction mixture was washed with saturated $NaHCO_3$ (8 mL) and brine (10 mL). The combined organics were dried over sodium sulfate and concentrated under reduced pressure. The product was purified by silica gel flash chromatography (5%-40% EtOAc/Hex gradient) to obtain the target compound **13** (128 mg, 0.24 mmol) in 21% yield. Characterization and spectra available.[25]

2.2.7 Synthesis of 1-((tert-butyldimethylsilyl)oxy)-1-((3aR,4S,6S,6aS)-6-(2,4-di-tert-butoxypyrimidin-5-yl)-2,2-dimethyltetrahydrofuro[3,4-d][1,3]dioxol-4-yl)-3,3-dimethylbutan-2-one

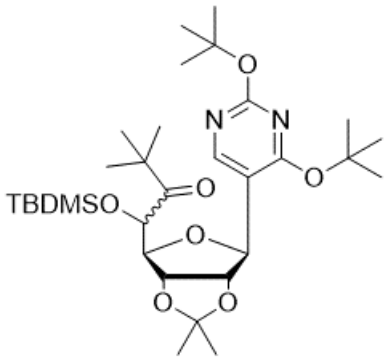

14

Compound **13** (108 mg, .20 mmol) was co-evaporated with toluene, and the flask subsequently equipped with a stir bar. The flask was purged with dry Argon gas, and compound **14** was dissolved in anhydrous THF. The solution was cooled to -78 °C and a *t*-BuLi solution (.48 mL, .81 mmol, 1.7 M solution) was added slowly and allowed to react 5 mins and before quenching with deionized water (3 ml). After allowing time to thaw, the solution was extracted with EtOAc (10 ml x 3). The organic layers were dried over sodium sulfate and concentrated under reduced pressure. The obtained residue was dissolved in ACN (4 ml) and water (2 ml) was added. Using 0.1N HCl, the solution was acidified to pH 5-6 and heated to 60 °C for 2 h. The reaction was monitored by TLC (40% EtOAc/Hex). After 2 h, the solution was extracted with EtOAc (10 ml x 3), and the combined organic layers dried over sodium sulfate before concentration under reduced pressure to obtain the crude product. The compound was purified using silica gel flash chromatography (5% to 30% EtOAc/Hex gradient) to obtain product **14** (13.6 mg, 0.02 mmol) in 10% yield.

HRMS $[M+H]^+$: calculated for $C_{27}H_{46}N_2O_7Si$ 595.3773, observed 595.3790

2.2.8 1-((3aR,4R,6S,6aS)-6-(2,4-di-tert-butoxypyrimidin-5-yl)-2,2-dimethyltetrahydrofuro[3,4-d][1,3]dioxol-4-yl)-1-hydroxy-3,3-dimethylbutan-2-one

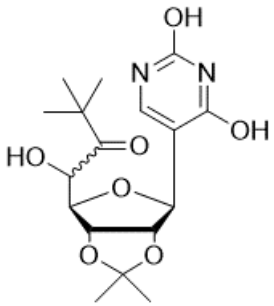

15

Compound **14** (13.5 mg, 0.023 mmol) was dissolved in THF (1 mL) with stirring. To this solution was added TBAF (0.035 mmol, 35 μL, 1M solution). Reaction was allowed to stir 4.5 h. After completion, purification was done by spotting reaction mixture onto a glass-backed preparative TLC plate and developed in 13% EtOAc/Hex.

Chapter 3

Discussion

3.1 Known methods for synthesizing pseudouridine

Several different approaches for the synthesis of pseudouridine have been developed over the past few decades, with some approaches yielding better results than others.[1, 2, 4, 26] Pseudouridine is an important biomolecule, and is relatively costly to obtain in larger amounts. This is due to the fact that historically, commercial suppliers isolated the compound from natural sources. Thus, there is a need for an efficient synthetic route to produce pseudouridine relatively cheaply in multi-gram quantities for use by researchers. Several groups have developed synthetic routes to accomplish this, which range in complexity and elegance.

One issue in synthesizing pseudouridine is the need for isomerically pure compounds, as the natural form of pseudouridine is the β isomer; the α isomer is biologically irrelevant. This means the synthesis needs to be stereoselective, or the isomers need to be separated in some manner. Previous approaches, as well as the advantages and disadvantages, are discussed in this section.

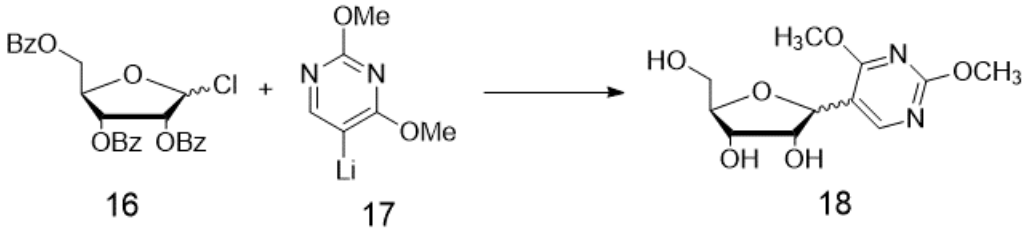

Figure 3-1 Synthesis of Pseudouridine by Shapiro et. al.

To our knowledge, all of the known approaches to pseudouridine have involved the same general pathway: the addition of a lithiated pyrimidinyl compound protected as alkyl ethers to a protected ribose derivative. This is followed by the appropriate deprotections to obtain pseudouridine. One of the earliest published syntheses for pseudouridine was by Shapiro et al. (**Figure 3-1**).[1] Their work involved the reaction of benzoylated ribofuranosyl chloride sugar **16** with a lithiated pyrimidinyl base protected as dimethyl ether **17**. The reported yield was 2% based on the sugar derivative. The low yield was attributed to the lack of sterospecificity resulting in the production of undesired isomers. An interesting side product was noted during acidic hydrolysis of the methoxy

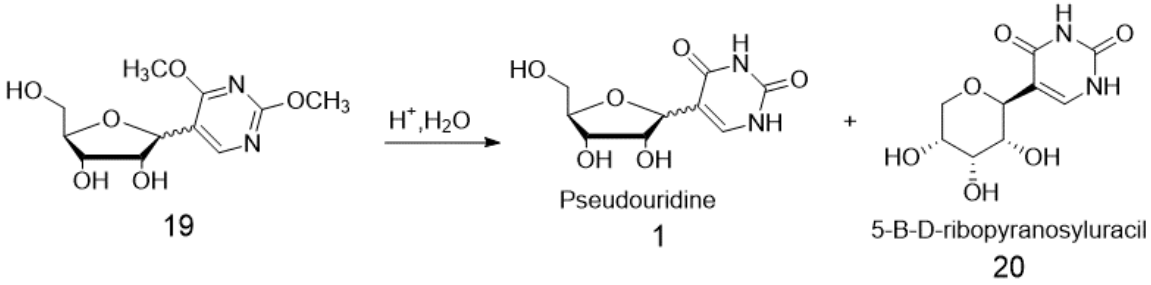

Figure 3-2 Acidic hydrolysis products observed by Shapiro et. al.[1]

protecting groups as well, which was determined to be 5-β-D-ribopyranosyluracil **20** (**Figure 3-2**).

Brown et al. reported an improved synthesis that involved using benzylated ribose and a *tert*-butoxy protected lithiated pyrimidinal base.[26] The *tert*-butoxy ethers are more susceptible to acid hydrolysis, which allows for less harsh conditions to be used in order to avoid the isomerization that was seen in the synthesis reported by Shapiro et al. Their approach resulted in a higher yield and no pyranose isomers.

Chow's group improved on this synthesis of pseudouridine by using a ribonolactone protected by 2′,3′-isopropylidene and 5′-TBDPS instead of benzylated ribose **21**(**Figure 3-3**).[2] This was coupled to lithiated pyrimidinyl compound **17** protected with methyl ethers. For the reduction step, BF_3-Et_2O was used with Et_3SiH. Two different approaches were used for the reduction with varying results. High equivalents of Et_3SiH (44 total) resulted in the removal of the isopropylidene protecting group (**24**), while a more modest 6 equivalents resulted in a 1:1 mixture of α/β isomers with the isopropylidene group intact (**23**). The former approach was believed to be better from a practical standpoint, and allowed for the isolation of the desired β-isomer in 20-35% yield. The isomers are more difficult to separate with the isopropylidene group intact, so the later approach necessitated removal of this group using acetic acid under reflux conditions. The base protecting groups were removed with NaI and acetic acid while methanolic HCl removed the 5′-TBDPS group. Reported overall yield was 20%.

Hanessian's group improved upon Chow's synthesis (**Figure 3-4**). Their work also began with protected ribonolactone **25**, however hydroxyl protection was achieved in a single step using 2,2-dimethoxypropane to form a bis-acetal. This was coupled with *tert*-butyl ether protected lithiated pyrimidinyl compound **27** as in Brown's work. The resulting compound (**28**) was reduced using L-selectride in the presence of zinc chloride, under conditions which favor the formation of the desired β-isomer. They found that the absence of zinc chloride gave a 20:1 mixture of α/β isomers, offering a high level of control over the stereochemistry of the product.

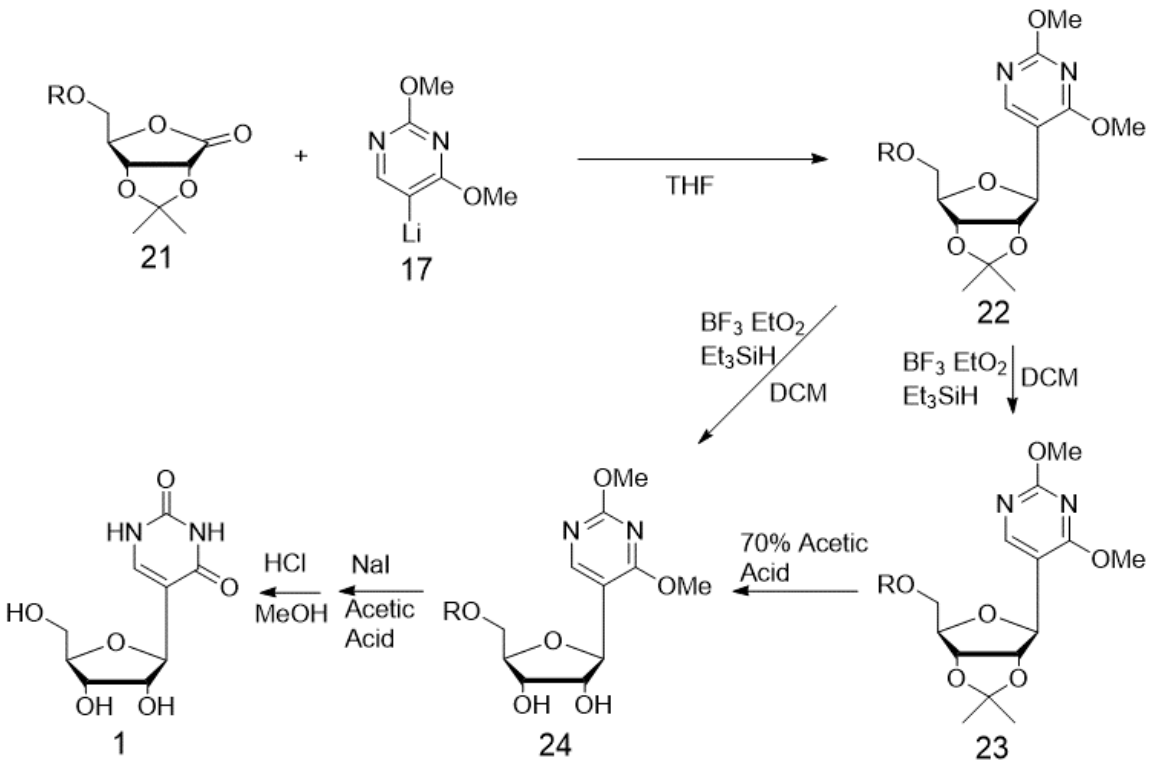

Figure 3-3 Synthesis of pseudouridine by Chow et al.[2] R=TBDPS

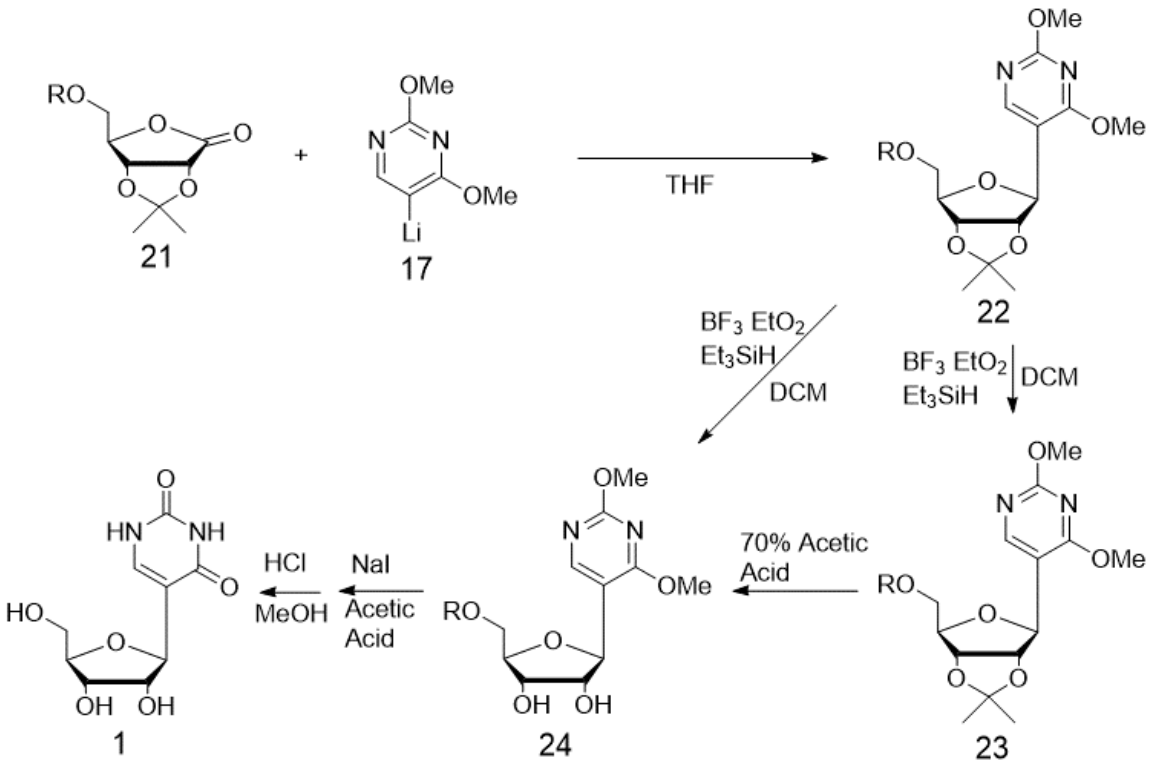

Figure 3-4 Synthesis of pseudouridine as reported by Hanessian et al. [4]

Zinc chloride acts by chelation with the ketone carbonyl and the acetal oxygen to allow hydride attack from the *si*-face (**Figure 3-5**). In the absence of this chelation, attack from the *re*-face is preferred as it is more exposed. A possible pathway for this reduction is outlined below.

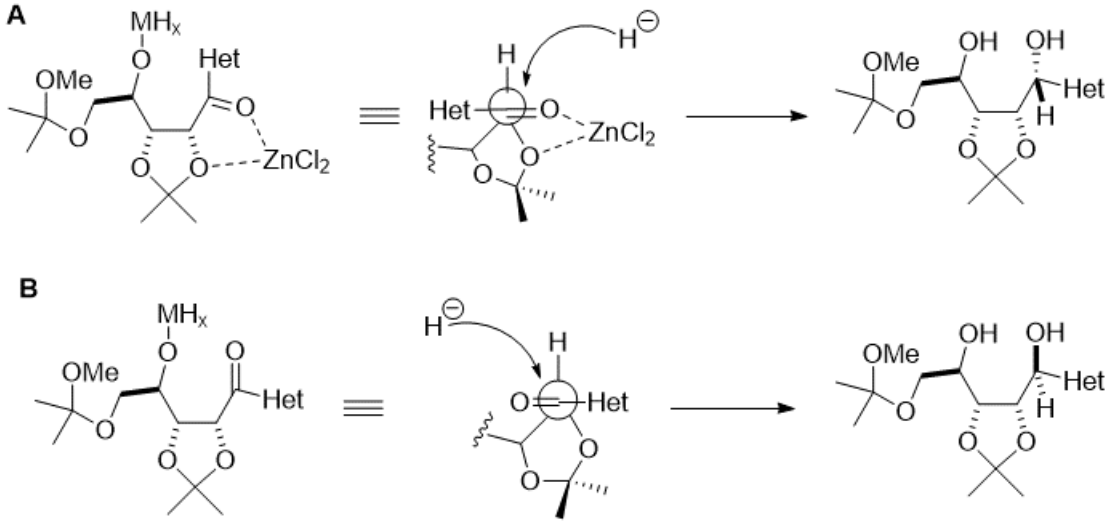

Figure 3-5 Stereoselective reduction pathway in work by Hanessian et. al. [4] A represents the result in the presence of $ZnCl_2$ while B shows the effect of its absence.

Following steroselective reduction, an intramolecular Mitsunobu reaction was used for cycloetherification of the sugar ring to obtain compound **30**, followed by an acid hydrolysis to achieve complete deprotection in a single step. This method allowed for a reported overall yield of 46% from the starting ribonolactone.

Hanessian's route to pseudouridine has proven to be the most efficient. The stereoselectivity achieved in this synthesis is much better than what was reported by other groups. The relatively cheap reagents needed for this synthesis allow for easy preparation of multigram quantities of pseudouridine. Our lab has attempted to replicate this synthesis, and has run into issues with the protecting group strategy. Specifically, it has been observed that achieving complete protection in one step is more difficult than it was reported to be. We also noticed lower yields than what has been reported. We used a different 5´-OH protecting group that may account for this difference due to the much larger size of the TBDPS group.

3.2 Known methods for synthesizing radical precursors

Radical induced damage in RNA has been shown to have consequences on the biological fate and function of the cell. There is a need then to try and model the damage that this important class of biomolecules is exposed to, in order to provide mechanistic insights into the effects of radical induced damage. Simply exposing the biomolecule to oxidative stress conditions would not provide information as to the fate of a radical at a specific position on a given nucleoside. In order to study the effects of radical damage at various specific positions on a given nucleoside, so-called radical precursor molecules have been synthesized. These molecules are made by synthetically introducing a photolabile group at a position of interest on the nucleoside. These groups undergo Norrish Type I photocleavage and homolytically cleave upon exposure to UV radiation with a wavelength of ≥320 nm (but <400 nm), which is in the biologically relevant UVA spectrum. This hemolytic cleavage results in the formation of a radical at the corresponding position allowing insights into the products formed from that radical, and a better mechanistic understanding of how the damage products are formed.

Radical precursor molecules of different types have been synthesized by several different groups, such as those of Giese[3, 27], Chatgilialoglu[28], Greenberg[29], and Bryant-Friedrich[25, 30]. Chatgilialoglu's group synthesized C5′-thymidine and C2′-guanosine radical precursors. Greenberg's group has synthesized C6, C5 and C2′-uridine radical precursors, while Giese's work has produced a 3′ and 4′-thymidine precursor. Our group has published C3′-thymidine. As the present work only pertains to sugar radical precursor, synthetic approaches to reach these molecules will be discussed here.

There are several different photolabile moieties that have been used successfully as radical precursors. Phenyl selenium derivatives have proven effective as a radical precursor molecules, as have several different carbonyl products. In their work on 3´-thymidine radical precursors, Giese's group synthesized and compared a methyl ketone, a *tert*-butyl ketone, and a benzoyl ketone.[3]

The synthetic route used to reach these molecules (**Figure 3-6**) was based on a known 3´-carbonyl compound **31**. Starting at the carbonyl, TMSCN was reacted in the presence of catalytic 18-crown-6 and KCN to form a TMS protected cyanohydrin **32**. The cyanohydrin was then subjected to nucleophilic addition with an alkyl lithium compound (methyl, *tert*-butyl, or phenyl lithium) to produce an intermediate imine, which was hydrolyzed to the corresponding ketone using 1N HCl. The radical precursor that resulted

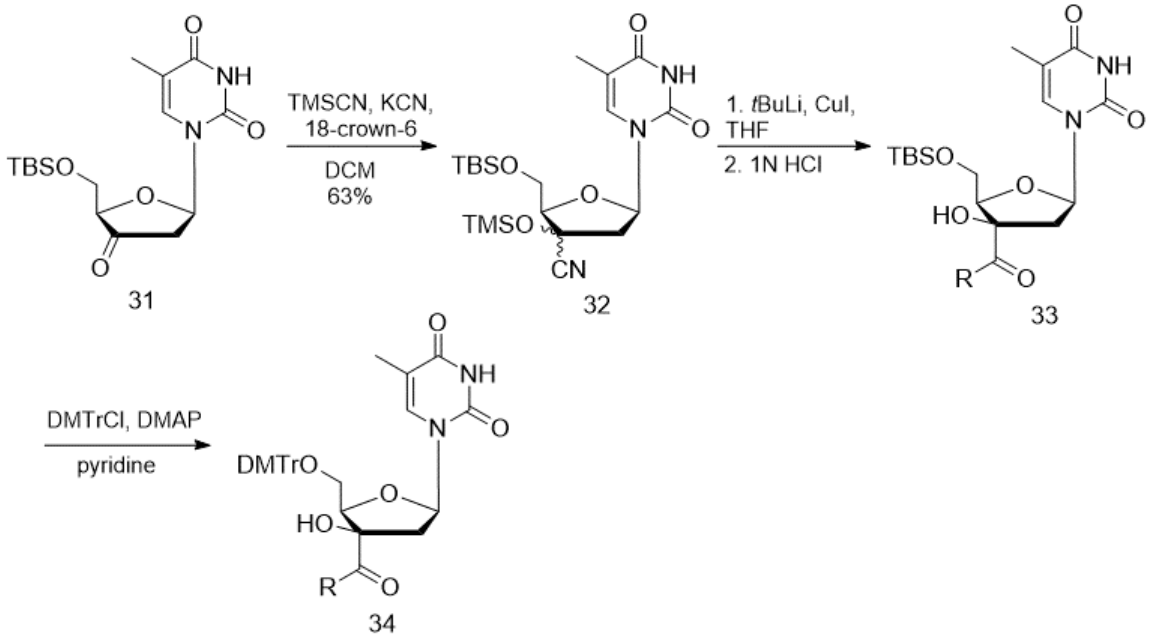

Figure 3-6 Synthesis of C3´-thymidine radical precursor **34** by Giese et. al. [3]

was then protected at the 5′-OH using the DMTr group by way of standard methods to obtain compound **34**.

To confirm the validity of these molecules as radical precursors, confirmatory photolysis studies were performed. The precursor molecule **34** was subjected to UV irradiation using wavelengths ≥320 nm in the presence of excess nBu_3SnH as a hydrogen atom donor (**Figure 3-7**). All three derivatives were subjected to photolytic conditions, and the yield of the expected tritylated thymidine recorded (**Table 3-1**). The *tert*-butyl ketone gave the cleanest results with the highest yield of expected product **37**. The 3′-β-methylketone gave undesired side products, likely due to Norrish type II photcleavage instead of the desired Norrish type I. The benzoyl ketones performed poorly, giving low yields of the desired reduction product.

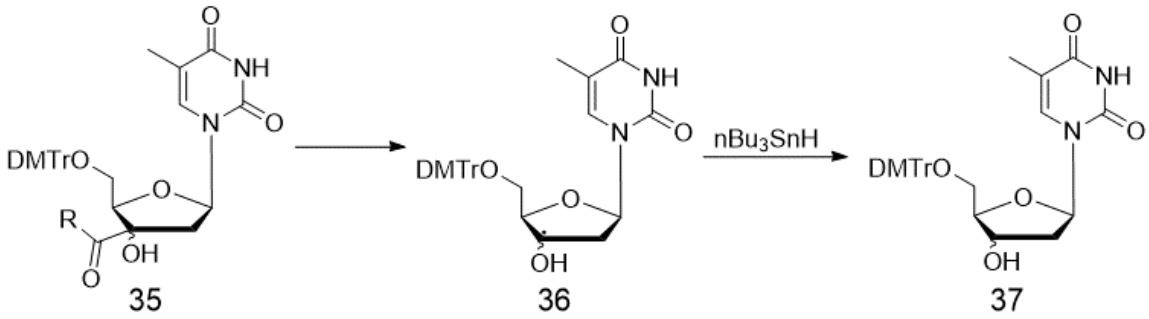

Figure 3-7 Photolysis of 3′-thymidine radical precursors by Giese et. al.

The confirmatory studies proved that the synthesized tert-butyl ketone of thymidine acted effectively as a radical precursor. The *tert*-butyl ketone was found to be the derivative most effective, and has been used by several research groups interested in radical induced damage in DNA.

Table 3-1 Photolysis yields and times for different precrusors from Giese et al. [3]

Ketone	Length of irradiation	Yield(%)
CH_3	3 h	20
CH_3	3 h	65
Ph	2 h	35
Ph	2 h	33
$(CH_3)_3C$	1 h	79
$(CH_3)_3C$	1 h	92

The group of Chatgilialoglu synthesized C5′ radical precursor derivatives of thymidine (**Figure 3-8**) and 2′-deoxyguanosine in their research into sugar radical damage in DNA.[23] Their synthetic pathway started by synthesizing the C5′ aldehyde **38** using known procedures. The aldehyde was then converted into cyanohydrin **39** as in the work on 3′-thymidine precursors by Giese. This cyanohydrin was reacted with *tert*-butyllithium to form a *tert*-butyl imine intermediate **40**, which characterized by NMR using acid-free solvents; exposure to chloroform-d resulted in

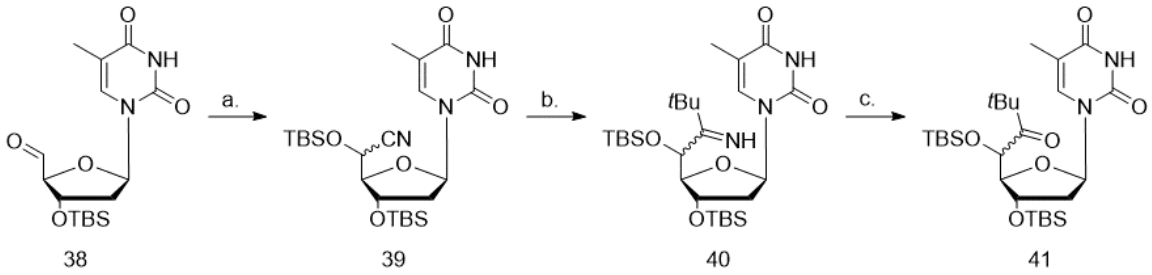

Figure 3-8 Synthesis of 5′-thymidine radical precursor by Chatgilialoglu et. al. a.) TBDMS-CN, LiOEt, THF, 82%; b.)*t*BuLi, THF, 43%; c.)THF/H_2O/ 2 N HCl, 88%

decomposition to unidentifiable fragments. The imine was hydrolyzed to the corresponding ketone **41** in excellent yield using a THF/water/2N HCl solution.

The approach used for the guanosine derivative was similar but necessitated use of different methods than those used in thymidine in several steps. The formation of the C5′ aldehyde was done by way of a modified Moffatt oxidation procedure and used EDC, pyridine, TFA, and toluene/DMSO (2:1) to achieve 95% conversion. The oxidation products presented as a mixture of three diastereomeric hemiacetals that form as hydration products of the aldehyde in aqueous solutions. This mixture was reacted with TBDMSCN in the presence of ZnI_2 to yield a 5′-cyanhydrin in the form of two diastereomers. The cyanohydrin isomers were exposed to *tert*-butyllithium to produce the *tert*-butyl imine as in the thymidine system. This compound was found to be stable to column chromatography, and could be isolated and characterized, though yields were still modest. Treating the imine with acetic acid/THF/water (4:1:1) led to the formation of the corresponding ketone in a reported yield of 78%.

Photolysis in the thymidine system (**Figure 3-9**) proceeded as expected, producing protected thymidine from the precursor molecule. Photolysis studies were also performed on the deprotected thymidine radical precursor **42**, resulting in the production of thymidine (**44**) as expected. The experiments were conducted in the presence of 1-butanethiol as a hydrogen donor in the case of the protected molecule, while more biologically relevant glutathione was used in the experiments performed on the deprotected precursor molecule (not shown).

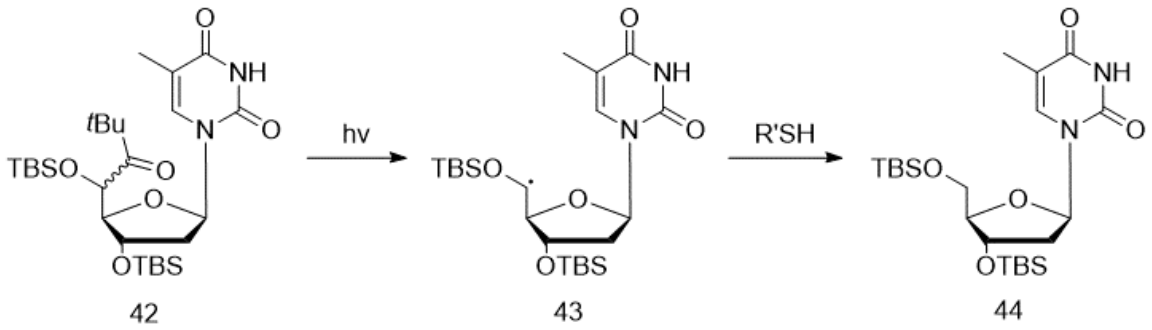

Figure 3-9 Photolysis of 5´-thymidine radical precursor **42** by Chatgilialoglu et al. [23]

Photolysis studies on the guanosine system in the presence of *t*BuSH as a hydrogen donor resulted in the formation of two distinctly different products (**Figure 3-10**). The first is guanosine derivative **46**, while the second is a cyclized compound **47**, (5´*S*)-5´,8-cyclo-2´-deoxyguanosine with no other diastereomeric products detected. The two different products are a result of competing pathways from the radical formed after photolytic cleavage of the *tert*-butyl ketone. The mechanism Chatgilialoglu proposed is shown below. They state that the cyclization product forms through a chair transition state leading to the 5´*S*,8*R* intermediate radical followed by rearomitization of the base through a reaction with the thiyl radical.[23] The high degree of stereoselectivity observed in the formation of this product is attributed to the steric hindrance between the 5´-O-TBDMS and the guanine moiety.

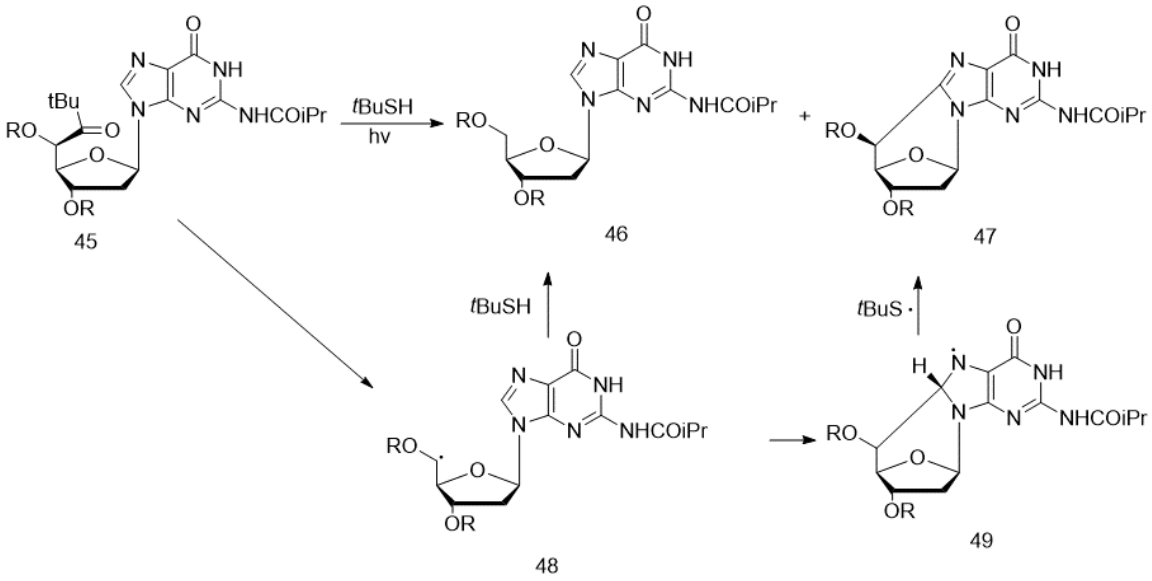

Figure 3-10 Photolysis product formation pathway in guanosine radical precursor from Chatgilialoglu et al.

The synthetic methods used by Chatgilialoglu's group to synthesize their thymidine and guanosine radical precursors are very similar to the methods used by Giese. The approach to synthesizing guanosine demonstrated another route to the cyanohydrin compound, and the imine was reported to exhibit excellent stability. The performed photolysis studies confirmed the validity of these molecules as radical precursors for studying radical damage at the C5´ position.

Greenberg et al. synthesized a 2´-uridinyl radical precursor molecule using a benzyl ketone as the photolabile moiety (**Figure 3-11**).[29] Upon photolysis, the only observed product was uracil; they state that this is in line with what was expected from

previous experiments, and further state that the 2´-uridinyl radical will induce nucleobase elimination very quickly.

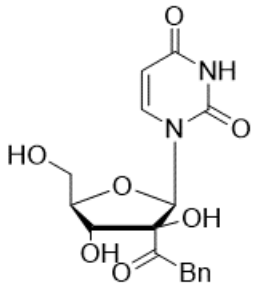

50

Figure 3-11 2´-uridinyl radical precursor synthesized by Greenberg et. al.

Our lab has also successfully synthesized radical precursors, including a 5´-uridinyl radical precursor.[31] The pathway to synthesize this molecule is very much similar to those used by Chatgilialoglu and Giese (**Figure 3-12**). The 5´-aldehyde was synthesized using the Dess-Martin periodinane without aqueous workup to prevent formation of the corresponding hydrate. Cyanohydrin formation occurred by way of the 18-crown-6/KCN approach. The cyanohydrin was then reacted with *tert*-butyllithium to form the *tert*-butyl imine, which was hydrolyzed using HCl in an ACN/water solution. The compound was deprotected using TBAF followed by 25% acetic acid under refluxing conditions to obtain the fully deprotected radical precursor. In the photolysis experiments, the major product observed was uracil, with only ~7-15% of the expected product, uridine, observed.

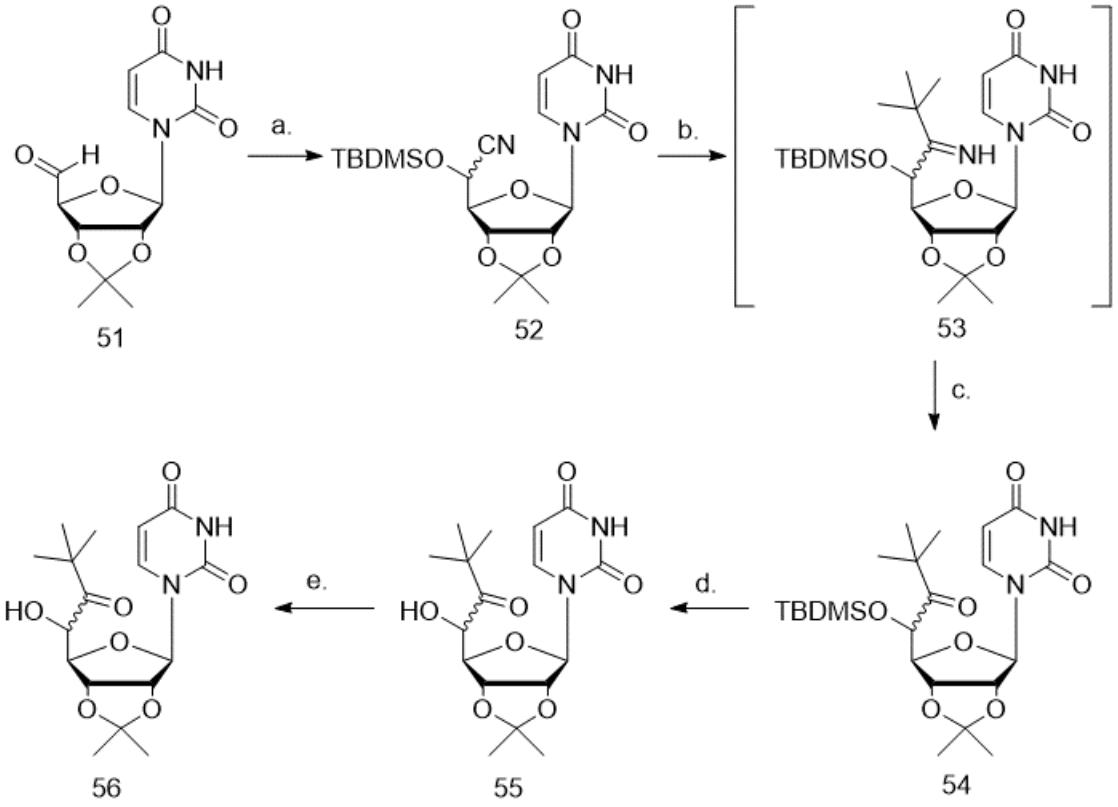

Figure 3-12 Synthesis of C5'-pivaloyl uridine a.) 18-crown-6, KCN, TBDMSCN, THF, 73%; b.)*t*BuLi, THF, -78 °C; c.) H_2O, 2 N HCl, 46%; d.) TBAF, THF, 84%; e.) 25% acetic acid, reflux, 94%

3.3 Synthetic approach in the present work

The synthetic route to our precursor (**Figure 3-13**) was inspired by work from Hannessian and Chows groups. Previous work in our lab resulted in the successful synthesis of cyanohydrin **13**, however the work progressed no further at that time.[25] A ribonolactone protected with 2′,3′-isopropylidene and a TBDPS group on the 5′-OH were utilized to obtain compound **57**.[32] This particular protecting group combination was chosen due to the ease of installation and the selectivity it affords; the 5'-TBDPS group can be removed without affecting the integrity of the other protecting groups in the molecule. Brominated pyrimidine compound **27** was protected with tert-butyl ethers [33] and attached to the protected sugar *via* nucleophilic addition utilizing *n*-butyllithium for lithium-halogen exchange. Due to the highly reactive nature of *n*-butyllithium, these

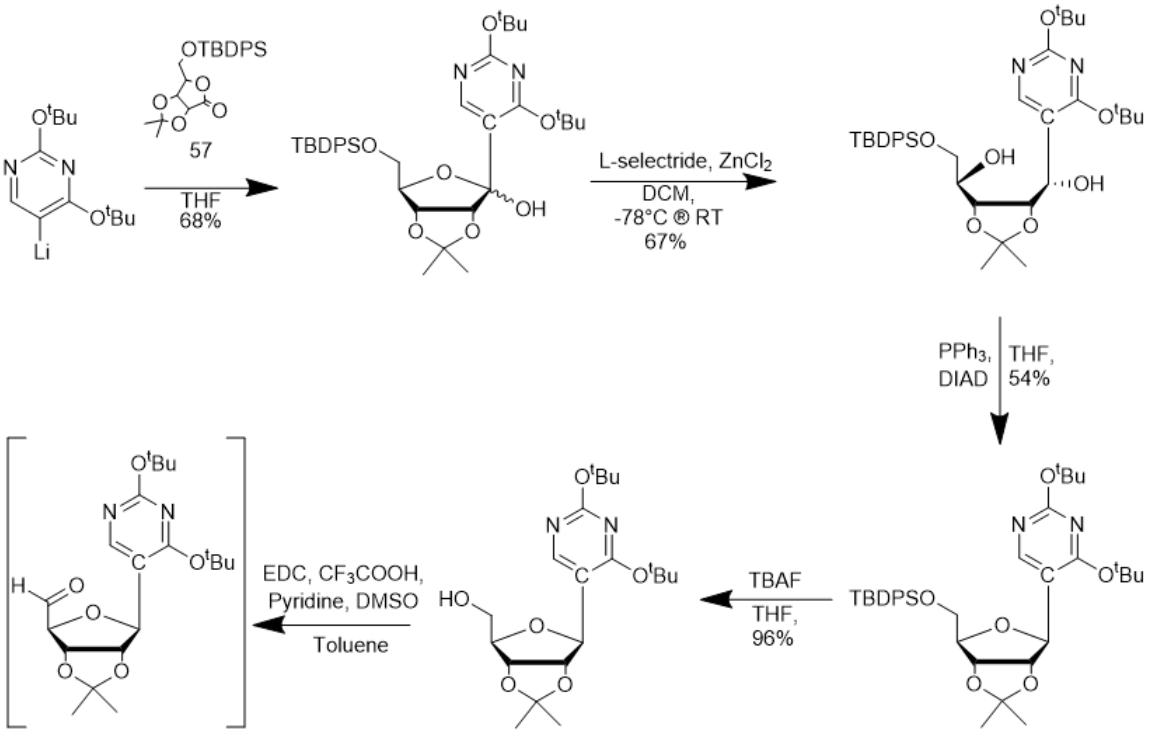

Figure 3-13 Synthetic route to aldehyde **12**

reactions were conducted at reduced temperatures for the duration of the reaction. The resulting product **8** is a mixture of isomers. To remove the 1′-OH, a steroselective reduction is utilized, followed by an intramolecular Mitsunobu reaction to give fully protected pseudouridine **10**. To achieve the stereoselective reduction, Hanessian's approach used L-selectride and zinc chloride at reduced temperature. The zinc chloride is added first, coordinates with the ribose ring (**Figure 3-14**) to allow the bulky L-selectride

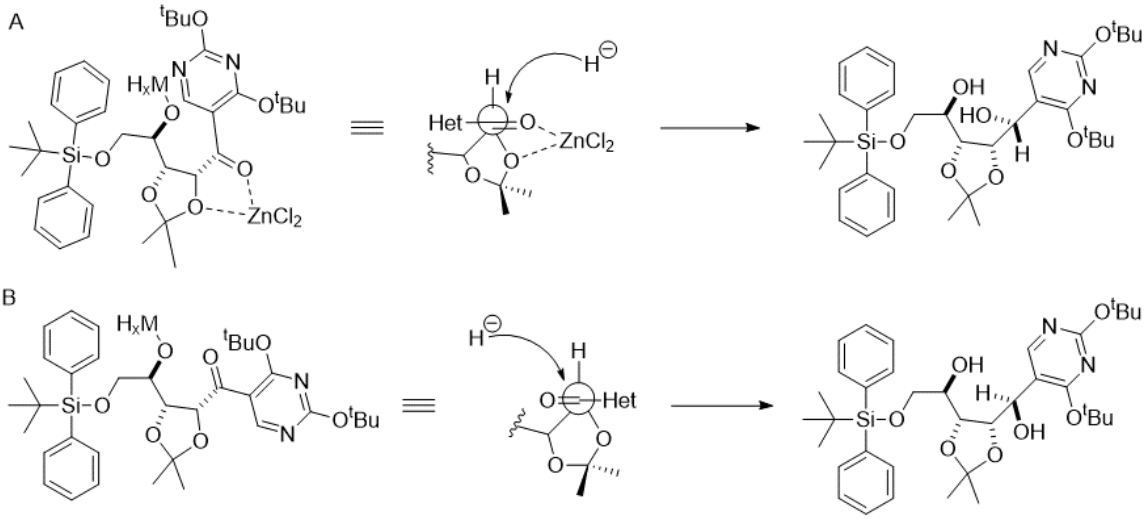

Figure 3-14 Depiction of the stereoselective reduction with L-selectride. A represents the result of the presence of $ZnCl_2$ while B shows the effect of its absence.

to deliver the hydride from one face, giving nearly complete conversion to the desired β-isomer.

Having synthesized fully protected pseudouridine, we used TBAF as a source of fluoride to remove the 5′-silyl ether protecting group to expose the 5′-OH while leaving the other hydroxyls protected. 5′-Alcohol **11** was oxidized to the corresponding aldehyde **12** by way of a modified Moffatt oxidation used by Chatgilialoglu in their synthesis of the 5′-guanosine precursor. Other methods of oxidation were tried here as well. The

Dess-Martin periodinane gave mixed results, and byproducts that were hard to remove. A Swern oxidation, which is a DMSO based oxidation, proved no better and was a less desirable approach due to the formation of toxic and pungent dimethylsulfide as a by-product. Due to the the fact that the aldehyde exists in equilibrium with its hydrate, it was found to be easier to use without further purification in reactions for conversion to the cyanohydrin (**Figure 3-15**). One of the more common approaches involves the use of catalytic 18-crown-6 in the presence of potassium cyanide and TMSCN or TBDMSCN, and several groups have had success with this approach to making 5´-cyanohydrin nucleosides. While this approach worked well in our groups work on uridine, very little product formation was observed in the pseudouridine derivative.[31] An alternative approach was investigated, using catalytic zinc iodide and TBDMS cyanide to give a protected 5´-cyanohydrin **13**. This approach resulted in increased yields compared to the 18-crown-6/ KCN approach, though yields were still modest at best and left room for improvement. It was also noticed that there is a modest formation of the 5´-OH cyanohydrin, where the TBDMS group failed to attach. Other approaches investigated

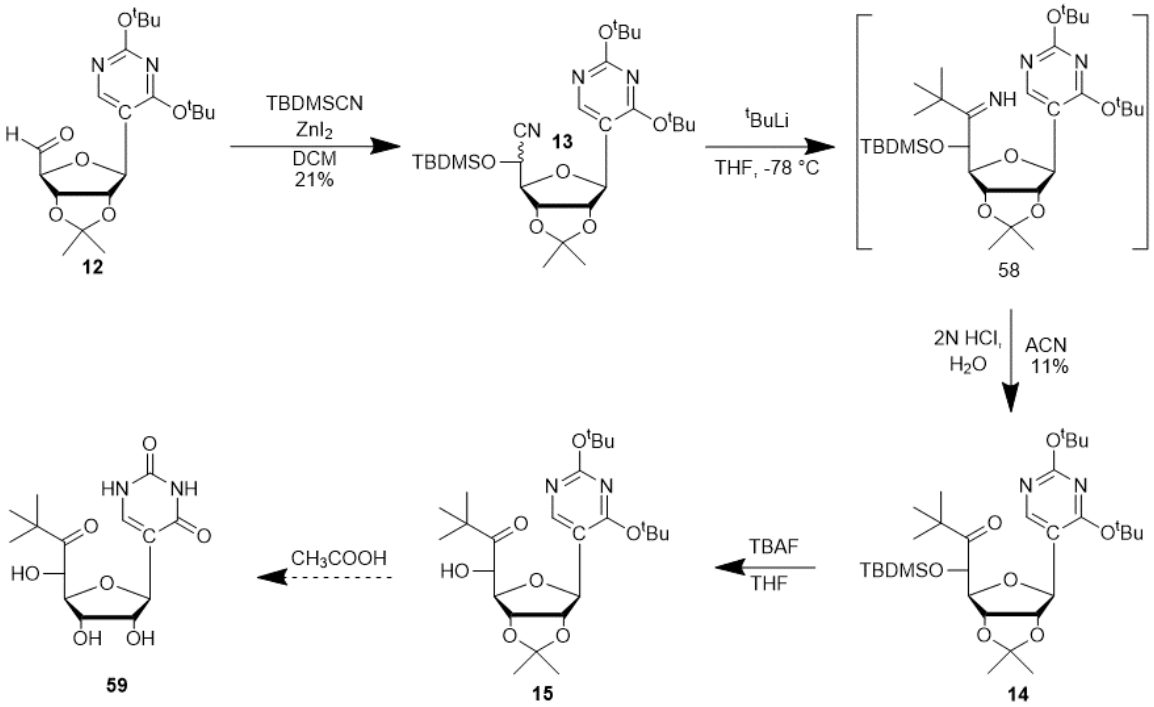

Figure 3-15 Synthetic route towards C5′-pivaloyl pseudouridine **59**

used TMSCN in place of TBDMSCN, but good yields were difficult to achieve and the TMS group exhibited extreme lability so the approach was abandoned.

The protected cyanohydrin acts as a wonderful synthetic intermediate, allowing us to quickly form *tert*-butyl imine **58** using *tert*-butyl lithium. Reaction times must be kept short as decomposition and reduced yields are likely if longer reaction times are used. The reaction mixture is concentrated and the imine is used without purification. The crude imine was exposed to acidic hydrolysis using acetonitrile acidified to pH5 using 1N HCl/ACN. Desired ketone **14** was formed and isolated, albeit in low yields. Having isolated the fully protected precursor, the 5′-TBDMS group was removed using TBAF in THF as a source of fluoride to obtain alcohol **15**. This compound was isolated using preparative TLC, and its identity confirmed by low-resolution mass spectrometry.

Multiple protecting group combinations were tried to see if changes had an effect on observed yields in the initial reactions (**Table 3-2**). We tried swapping the *tert*-butyl ether protecting groups on the base for the simpler and smaller methyl ether. Also attempted was a swap of the bulky TBDPS 5′-OH protecting group for a smaller TBDMS group. It was found that the TBDPS group combined with the *tert*-butyl ether was slightly more desirable from a practical standpoint. The bulky, non-polar nature of the phenyl and *tert*-butyl groups resulted in lower affinity to silica gel, which resulted in easier purification of the corresponding products.

Table 3-2 Protecting group, reagent selection and resulting yields

R_1	R_2	BuLi Cmpd.	Equivalents of Base	Yield
TBDPS	*t*Bu	nBuLi	2	68%
TBDPS	*t*Bu	tBuLi	2	None
TBDMS	Me	nBuLi	1.1	24%
TBDPS	Me	tBuLi	1.1	33%
TBDPS	Me	nBuLi	1.1	49%

It was found that the main difficulty in this synthesis, especially within the first few reactions, was an incredible sensitivity to moisture. Reactions that used THF, as a result, necessitated the use of freshly distilled solvent handled under inert conditions and careful drying of glassware. Solvent that was only modestly dry resulted in greatly diminished yields. This sensitivity also meant that starting materials had to be very dry, necessitating long dry times under high vacuum and in some cases co-evaporation to remove any traces of moisture still present.

The synthesis we have presented here is the most direct route to the target compound. Several low yielding reactions in the scheme make synthesizing large amounts of compound a challenge that still must be overcome. Room for improvement still remains in the synthetic route, in particular the formation of the cyanohydrin compound which proved difficult to synthesize in a good yield. The yield of the acid hydrolysis leaves room for improvement as well, perhaps more acidic conditions could provide a better yield of the ketone. Careful control of the pH is necessary, however, due to the acid labile protecting groups whose removal would make purification of the product difficult.

Chapter 4

Conclusion

We were able to synthesize the fully protected pseudouridine radical precursor in milligram amounts. The compound is the first radical precursor derivative of pseudouridine that has been synthesized to our knowledge. It represents an important molecule due to the ubiquity of pseudouridine in various species of RNA, such as tRNA and rRNA, which are longer lived than other forms of RNA and thus are more susceptible to oxidative damage. The synthetic route presented here has proved valid, though room for improvement still remains in several key transformations in the later stages of the synthesis. Regardless, this molecule represents a significant advancement in the field of RNA oxidation research due to its novel structure, and will allow us to determine what affect oxidative stress has on pseudouridine, and what affect the presence of pseudouridine in RNA has on the outcome of oxidative damage events.

Chapter 5

Future Work

5.1 Further optimization of the synthesis

Optimization of the key synthetic steps in the later stages of the synthesis is going to be necessary, in particular the cyanohydrin formation step and the formation of the *tert*-butyl ketone. There are other strategies for synthesizing cyanohydrins that have not been explored. Lowering the pH further during the acidic hydrolysis of the imine is an option, though literature suggests strongly acidic conditions can cause pseudouridine to isomerize to the pyranose form, and loss of protecting groups is a possibility under highly acidic conditions as well.

5.2 Monomer photolysis studies

To prove that our radical precursor is effective as a radical precursor, photolysis studies will be conducted on the fully deprotected monomer under aerobic and anerobic conditions, in the presence of a hydrogen donor. The outcome of this should be the formation of pseudouridine, though research in uridine yielded a large amount of the base elimination product.[31] It will be interesting to compare the difference in stability of the

sugar-base bond between the C-N and C-C structural isomers of uridine and pseudouridine.

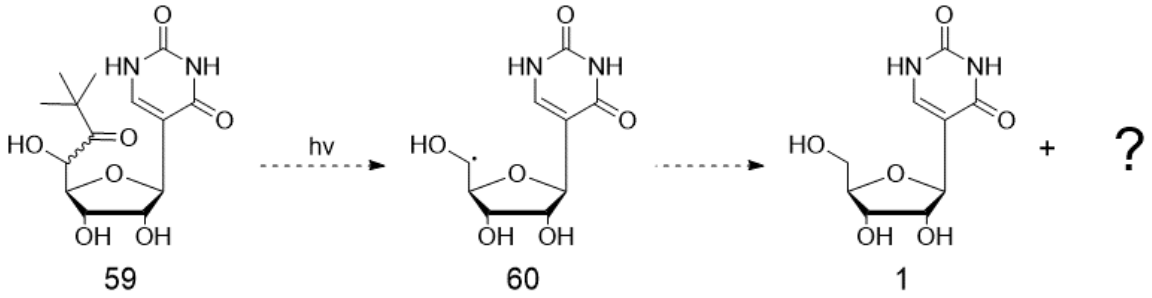

Figure 5-1 Proposed scheme for the photolysis of compound **59** monomer

Analysis of the photolysis samples will be conducted using HPLC with a UV/Vis detector as tandem LC/MS techniques. A reference sample of pseudouridine will be obtained and used to help determine if the expected outcome was achieved, as well as to provide the ability to make a calibration curve in order to quantify product formation.

The results of this study should confirm the validity of the molecule as an effective radical precursor and give interesting insights into the effects of radical damage to *C*-nucleoside analogues.

5.3 Derivatization for automated oligonucleotide synthesis

The ultimate goal of this project is to incorporate our pseudouridinyl radical precursor into biologically relevant oligonucleotides, which have yet to be chosen. This would allow us to determine what effect oxidative insult has on pseudouridine and the oligonucleotide. Photolysis of oligonucleotides can be conducted under aerobic and

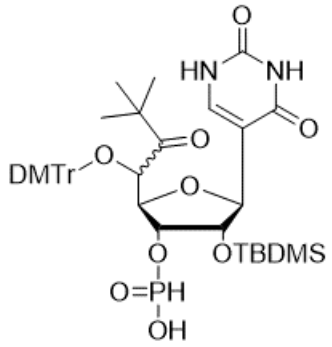

61

Figure 5-2 Proposed H-phosphonate derivative for automated oligonucleotide synthesis

anaerobic conditions, and the use of LC/MS-MS and MALDI-TOF mass spectrometry will allow the identification of any damage products that are formed. This would allow for unprecedented mechanistic insights into the outcome of an oxidative event that would generate a C5′ free radical. We propose an H-phosphonate derivative **61** as the best choice for oligonucleotide synthesis, as the steric issues created by the presence of a 5′-pivaloyl group makes success using the phosphoramidite approach unlikely. The synthetic approach to making this derivative has yet to be determined.

References

1. Shapiro, R.C., R.W., *Synthesis of Pseudouridine.* J. Amer. Chem. Soc., 1961. **83**(18): p. 3920-3921.

2. Grohar, P.J.C., C.S., *A Practical Synthesis of the Modified RNA Nucleoside Pseudouridine.* Tetrahedron Letters, 1999. **40**: p. 2049-2052.

3. Körner, S.B.-F., A.; Giese, B., *C-3'-Branched Thymidines as Precursors for the Selective Generation of C-3'-Nucleoside Radicals.* J. Org. Chem, 1999. **64**: p. 1559-1564.

4. Hanessian, S. and R. Machaalani, *A highly stereocontrolled and efficient synthesis of α- and β-pseudouridines.* Tetrahedron Letters, 2003. **44**(45): p. 8321-8323.

5. Sheng Li, C.E.M., *The Pivotal Regulatory Landscapes of RNA Modifications.* Annu. Rev. Genom. Human Genet., 2014. **15**: p. 127-150.

6. Satterlee, J.S., et al., *Novel RNA modifications in the nervous system: form and function.* J Neurosci, 2014. **34**(46): p. 15170-7.

7. Meier, U.T., *Pseudouridylation goes regulatory.* EMBO J, 2011. **30**(1): p. 3-4.

8. Wang, X. and C. He, *Dynamic RNA modifications in posttranscriptional regulation.* Mol Cell, 2014. **56**(1): p. 5-12.

9. Gray, M.C.a.M., *Pseudouridine in RNA: What, Where, How, and Why.* Life, 2000. **49**: p. 341-351.

10. Jack, K., et al., *rRNA pseudouridylation defects affect ribosomal ligand binding and translational fidelity from yeast to human cells.* Mol Cell, 2011. **44**(4): p. 660-6.

11. Luca, M., A. Luca, and C. Calandra, *The Role of Oxidative Damage in the Pathogenesis and Progression of Alzheimer's Disease and Vascular Dementia.* Oxid Med Cell Longev, 2015. **2015**: p. 504678.

12. Holbrook, T.F.a.N.J., *Oxidants, oxidative stress and the biology of ageing.* Nature, 2000. **408**(9): p. 239-247.

13. Abe, J.B., B.C., *Reactive Oxygen Species as Mediators of Signal Transduction in Cardiovascular Disease.* Trends in Cardiovascular Med. , 1998. **8**: p. 59-64.

14. Castellani, R.J., et al., *Sublethal RNA oxidation as a mechanism for neurodegenerative disease.* Int J Mol Sci, 2008. **9**(5): p. 789-806.

15. Li, J., et al., *Oxidative stress and neurodegenerative disorders.* Int J Mol Sci, 2013. **14**(12): p. 24438-75.

16. Wurtmann, E.J. and S.L. Wolin, *RNA under attack: cellular handling of RNA damage.* Crit Rev Biochem Mol Biol, 2009. **44**(1): p. 34-49.

17. Nunomura, A., et al., *Oxidative damage to RNA in aging and neurodegenerative disorders.* Neurotox Res, 2012. **22**(3): p. 231-48.

18. Nunomura, A., et al., *Oxidative damage to RNA in neurodegenerative diseases.* J Biomed Biotechnol, 2006. **2006**(3): p. 82323.

19. Li, Z., et al., *Battle against RNA oxidation: molecular mechanisms for reducing oxidized RNA to protect cells.* Wiley Interdiscip Rev RNA, 2014. **5**(3): p. 335-46.

20. Nunomura, A., et al., *RNA oxidation in Alzheimer disease and related neurodegenerative disorders.* Acta Neuropathol, 2009. **118**(1): p. 151-66.

21. Jacobs, A.C., M.J. Resendiz, and M.M. Greenberg, *Product and mechanistic analysis of the reactivity of a C6-pyrimidine radical in RNA.* J Am Chem Soc, 2011. **133**(13): p. 5152-9.

22. Newman, C.A., et al., *Photochemical generation and reactivity of the 5,6-dihydrouridin-6-yl radical.* J Org Chem, 2009. **74**(18): p. 7007-12.

23. Antonio Manetto, D.G., Leondios Leondiadis, Thanasis Gimisis, Peter Mayer, Thomas Carell, Chryssostomos Chatgilialoglu, *Independent Generation of C5'-Nucleosidyl Radicals in Thymidine and 2'-Deoxyguanosine.* J. Org. Chem, 2007. **72**: p. 3659-3666.

24. Ingle, S., et al., *Chemical probing of RNA with the hydroxyl radical at single-atom resolution.* Nucleic Acids Res, 2014. **42**(20): p. 12758-67.

25. Shaik, R., *Photochemical Generation of the C5' -Uridinyl and Pseudouridinylradical for the Study of Oxidative Damage in RNA*. 2013, University of Toledo: Department of Chemistry. p. 155.

26. Brown, D.M.O., R.C., *A Synthesis of Pseudouridine.* J. Chem. Soc. Perk. Trans I, 1981. **1**: p. 723-725.

27. Schiemann, O., et al., *4'-pivaloyl substituted thymidine as a precursor for the thymyl radical: an EPR spectroscopic study.* Chemphyschem, 2004. **5**(2): p. 270-4.

28. Manetto, A.G., D.; Leondiadis, L.; Gimisis, T.; Mayer, P.; Carell, T.; Chatgilialoglu, C., *Independent Generation of C5'-Nucleosidyl Radicals in Thymidine and 2'-Deoxyguanosine.* J. Org. Chem, 2007. **72**: p. 3659-3666.

29. Paul, R. and M.M. Greenberg, *Independent generation and reactivity of uridin-2'-yl radical.* J Org Chem, 2014. **79**(21): p. 10303-10.

30. Audat, S.A., et al., *Synthesis of C3' modified nucleosides for selective generation of the C3'-deoxy-3'-thymidinyl radical: a proposed intermediate in LEE induced DNA damage.* J Org Chem, 2012. **77**(8): p. 3829-37.

31. Shaik, R.E., M.W.; Starr, M.J.;Amato, N.J.; Bryant-Friedrich, A.C., *Photochemical Generation of a C5'-Uridinyl Radical.* Chembiochem, 2015. **16**: p. 2379-2384.

32. Sasaki, S.T., Y.; Takahashi, R.; Senko, Y.; Kodama, K.; Nagatsugi, F.; Maeda, M., *Selective Formation of Stable Triplexes Including a TA or a CG Interrupting Site with New Bicyclic Nucleoside Analogues (WNA).* J Am Chem Soc, 2004. **126**: p. 516-528.

33. Kofink, C.C.K., P. , *Synthesis of Functionalized Diarylmethanes via a Copper-Catalyzed Cross-Coupling of Arylmagnesium Reagents with Benzylic Phosphates.* Org. Lett, 2006. **8**(18): p. 4121-4124.

Appendix

HRMS Spectra

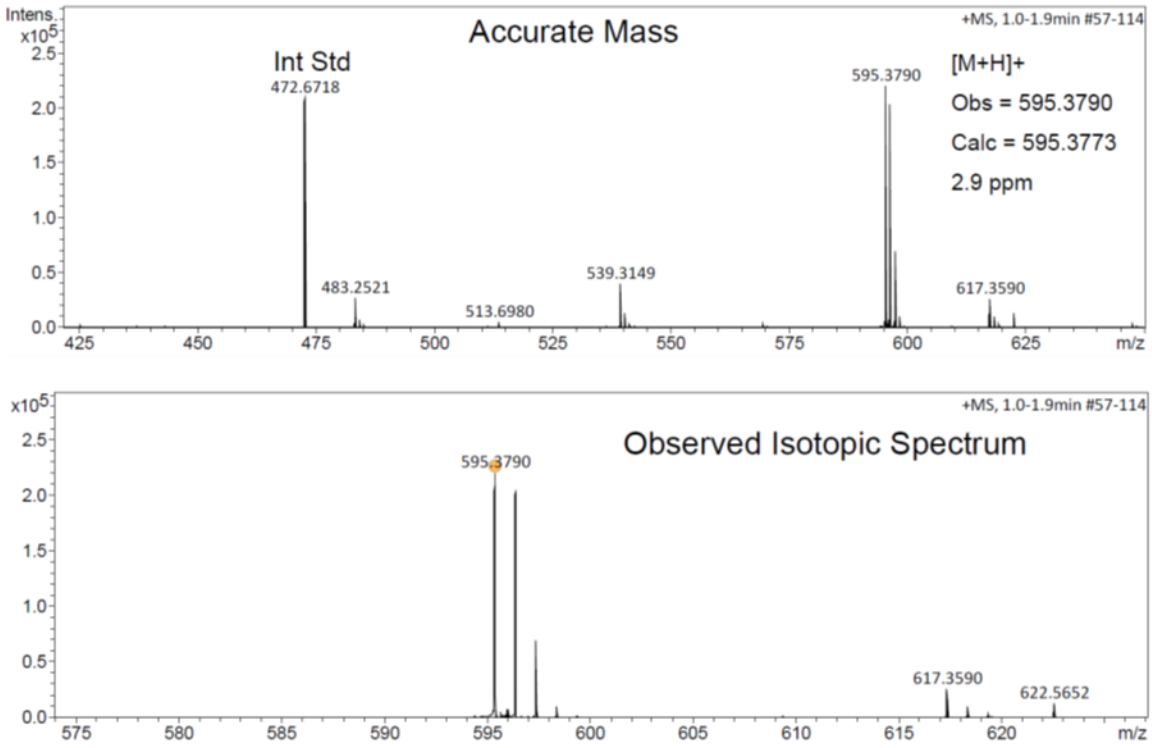

Figure A-3 HRMS analysis of Compound 10